Review

D. N. Basov*, Ana Asenjo-Garcia, P. James Schuck, Xiaoyang Zhu and Angel Rubio

Polariton panorama

https://doi.org/10.1515/nanoph-2020-0449
Received August 5, 2020; accepted October 2, 2020;
published online November 11, 2020

Abstract: In this brief review, we summarize and elaborate on some of the nomenclature of polaritonic phenomena and systems as they appear in the literature on quantum materials and quantum optics. Our summary includes at least 70 different types of polaritonic light–matter dressing effects. This summary also unravels a broad panorama of the physics and applications of polaritons. A constantly updated version of this review is available at https://infrared.cni.columbia.edu.

Keywords: portions; quantum electrodynamics; quantum materials; quantum optics.

Polaritons are commonly described as light–matter hybrid quasiparticles. Polaritons inherit their attributes from both their light and matter constituents. More rigorously, a polariton is a quantum mechanical superposition of a photon with a matter excitation, the latter being a collective mode in solids and superconducting circuits or an electron in atoms, molecules or even superconducting qubits. As such, the notion of polaritons is a unifying universal concept between the fields of quantum materials (QMs) and quantum optics/electrodynamics. Until fairly recently, these subfields of contemporary physics evolved largely independently of each other. Among the unintended consequences of these divisions is the ambiguity in polaritonic terminology with the same terms used markedly differently in QMs and cavity quantum electrodynamics (QED) with atomic systems. Here, we attempt to summarize (in alphabetical order) some of the polaritonic nomenclature in the two subfields. We hope this summary will help readers to navigate through the vast literature in both of these fields [1–520]. Apart from its utilitarian role, this summary presents a broad panorama of the physics and technology of polaritons transcending the specifics of particular polaritonic platforms (Boxes 1 and 2). We invite readers to consult with reviews covering many important aspects of the physics of polaritons in QMs [1–3], atomic and molecular systems [4], and in circuit QED [5, 6], as well as general reviews of the closely related topic of strong light–matter interaction [7–11, 394]. A constantly updated version is available at https://infrared.cni.columbia.edu.

Anderson–Higgs polaritons [12, 13]. The matter constituent of these polaritons originates from the amplitude mode in superconductors [14] (Figure 1). Anderson–Higgs polaritons are yet to be experimentally observed.

Bardasis–Schrieffer polaritons. The matter constituent of Bardasis–Schrieffer (BaSh) polaritons is associated with the fluctuations of subdominant order parameter in superconductors [15, 16], charge density wave systems [13], and excitonic insulators [17]. This novel theoretical concept still awaits experimental confirmation. The requisite experiments include nanospectroscopy and nanoimaging of polaritonic dispersion in the terahertz (THz) frequency range below the energy gap of superconductors. These are challenging scanning probe measurements, as they have to be carried out at cryogenic temperatures. Nano-THz imaging at cryogenic temperatures have been recently fulfilled [18], paving the wave to the exploration of polaritonic phenomena in superconductors (see also *Cooper pair plasmon polaritons* and *Josephson plasmon polaritons*).

Berreman polaritons: Phonon polaritons in anisotropic materials and multilayer structures are also referred to as epsilon-near-zero or *ENZ polaritons* [29–31]. ENZ materials, artificial structures, and nanocavities reveal exotic electromagnetic responses with a broad range of technological applications [31–35]. For example, ENZ nanocavities facilitate ultrastrong coupling between plasmonic and phononic modes [36], as well as the so-called photonic doping [37].

Berry plasmon polaritons: chiral plasmonic modes whose dispersion is explicitly impacted by the Berry curvature and

*Corresponding author: D. N. Basov, Department of Physics, Columbia University, New York, NY 10027, USA, E-mail: db3056@columbia.edu
Ana Asenjo-Garcia, Department of Physics, Columbia University, New York, NY 10027, USA
P. James Schuck, Department of Mechanical Engineering, Columbia University, New York, NY 10027, USA
Xiaoyang Zhu, Department of Chemistry, Columbia University, New York, NY 10027, USA
Angel Rubio, Max Planck Institute for the Structure and Dynamics of Matter, Luruper Chaussee 149, 22761 Hamburg, Germany; and Center for Computational Quantum Physics (CCQ), Flatiron Institute, 162 Fifth Avenue, New York, NY 10010, USA

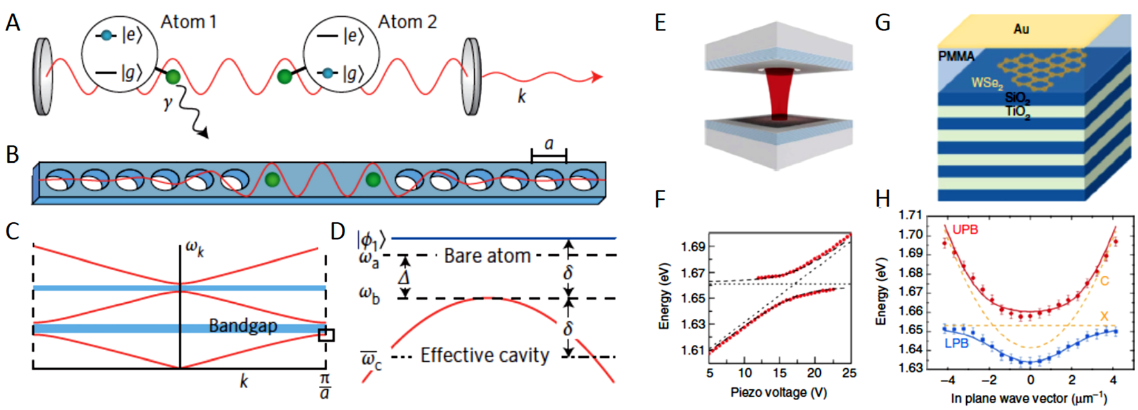

Box 1: Cavity quantum electrodynamics and cavity polaritons. In cavity quantum electrodynamics (QED), the spontaneous emission of atoms, molecules, and solids is governed not only by the properties of the emitter *per se* but is also controlled by its local electromagnetic environment. Optical cavities assembled from two parallel mirrors have long been used to confine light, to enhance light–matter interaction and to promote lasing [19]. The probability of interaction between light and matter is enhanced by the number of bounces the photon makes between the mirrors before leaving the cavity, which is conventionally quantified by the cavity finesse *F*. Cavities with high quality factors promote extremely efficient light matter couplings. In the strong-coupling regime (where the coherent interactions between the matter excitation and the cavity mode overcome the dissipation, i.e., when the vacuum Rabi splitting is much larger than the linewidth), the atomic or material excitation hybridizes with the photonic mode and produces a cavity polariton. The minimum separation upper polariton branch and lower polariton branch $E_{UPB}-E_{LPB}$ in Panel H is commonly referred to the normal-mode splitting in analogy to the Rabi splitting of a single-atom cavity system [20] (also Figure 4). Rabi splitting can reach fractions of eV in QMs and can exceed 1 eV in molecules [21, 22]. Strong coupling leads to photon blockade, where the presence of a photon in a cavity blocks a second one from coming in the study by Tian and Carmichael [23] and Imamoğlu et al. [24]. See also *microcavity polaritons*.
Panel A: cavity-mediated coherent interactions between two atoms in a Fabry–Perot resonator. Two atoms are coupled with strength g_c to a single mode of a Fabry–Perot cavity, enabling an excited atom (atom 1) to transfer its excitation to atom 2 and back. The coherence of this process is reduced by dissipation in the form of the cavity decay at a rate κ and atomic spontaneous emission into free space at a rate γ (adapted from a study by Douglas et al. [25]). Panel B is the photonic crystals, dielectric materials with a periodic modulation of their refractive index, which provide a rich playground for realizing tailored atom–atom interactions. Photonic crystals act as cavities that localize photonic modes (red) at defect sites, created by altering the periodicity (here, by removing certain holes). Atoms coupled to such a system may then interact via this mode in a manner analogous to that in A. Panel C is a typical band structure of a one-dimensional photonic crystal, illustrating the guided mode frequency ωk versus the Bloch wavevector k in the first Brillouin zone. Photonic crystals allow for the exploration of waveguide QED, where atoms are coupled to a propagating photon. Atoms coupled to the crystal have resonance frequency ωa close to the band edge frequency ωb, with $\Delta \equiv \omega a - \omega b$ (adapted from a study by Douglas et al. [25]). Panel D presents the effective cavity mode properties and energy level diagram for the photonic crystal dressed state $|\phi 1\rangle$ (blue), provided the atomic resonance lies inside the bandgap (a frequency region that does not support photon propagation). An excited atom hybridizes with the photonic mode giving rise to an atom–photon bound state, where the photon is localized around the atom, effectively forming a cavity. The dressed state energy ω is detuned by δ from the band edge into the bandgap (band shown in red). The atom is coupled to an effective cavity mode with frequency $\omega c = \omega b - \delta$ formed by superposition of modes in the band (adapted from a study by Douglas et al. [25]). Panel E is an open cavity based on two separated distributed Baragg reflector (DBR) mirrors (shaded blue). The monolayer of active semiconductor material (dark gray) is located on top of the bottom mirror [26]. Panel F is the distance between the mirrors in panel E which can be controlled by a piezo actuator, enabling the tuning of the optical cavity mode into resonance with the excitonic transition. The net effect is the observation of the anticrossing at resonance between the excitonic band and the cavity mode. Adapted from a study by Dufferwiel et al. [26]. Panels G and H are hybrid DBR microcavity with thin semitransparent metallic mirror on top [27]. The lower and upper polariton branches are observed. Trace C displays the cavity resonance C and line X marks the exciton resonance in the absence of coupling. Similar results for strong light–matter coupling in MoS_2 semiconductor integrated in DBR cavity were originally reported in a study by Liu et al. [28].

anomalous velocity in chiral media [38–40]. Berry plasmon polaritons are yet to be experimentally observed.

Bose–Hubbard polaritons: cavity QED polaritons with matter component associated with transitions across the Mott gap in the system of interacting atoms [41] (see also *Mott polaritons*).

Bragg polaritons. Bragg reflectors (Box 1 panel G, Figures 2 and 4) are routinely utilized to implement polaritonic cavities. Bragg polaritons pertain to systems in which multiple excitonic layers and/or quantum wells are periodically integrated in a DBR cavity [47, 48] (see also *polaritonic lattices*). The inherent anisotropy of Bragg

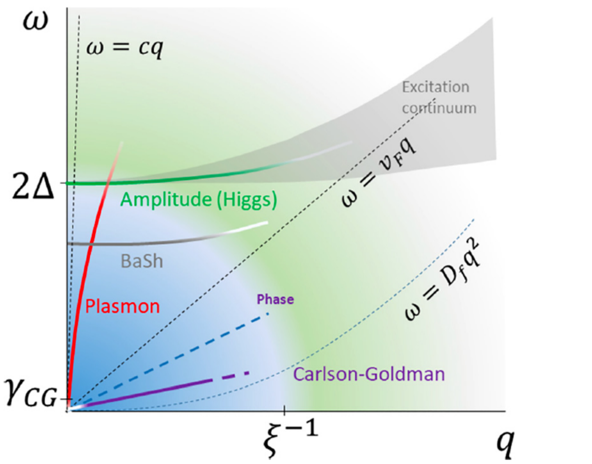

Figure 1: Schematic representation in the frequency–momentum plane of the collective modes that may appear in the electrodynamical response of a two-dimensional (2D) superconductor. The blue area shows the low-energy and long-wavelength region, where weakly damped collective modes may be observed. Anticrossing between the plasmon and Higgs mode and the Bardasis–Schrieffer (BaSh) mode is not shown here. Here, c is the speed of light, v_F is the Fermi velocity, and Df is the normal-state diffusion coefficient. Adapted from a study by Sun et al. [13].

multilayer structures may enable hyperbolic electrodynamics [49] (see *hyperbolic polaritons*).

Cavity (microcavity) polaritons. Weisbuch et al. [142] devised and implemented the first semiconductor (micro) cavity device revealing Rabi splitting of exciton polaritons (Boxes 1 and 2). Semiconductor microcavites emerged as a powerful platform for the investigation of strong light–matter interaction in semiconductors [50, 51]. Microcavity structures reveal intriguing phenomena including polariton parametric amplification [52] and its spontaneous counterpart, the parametric photoluminescence [53]. Parametric photoluminescence is a purely quantum process. An appealing attribute of polariton parametric photoluminescence is that signal-idler polariton pairs are produced in nonclassical states with quantum correlations. The quest for Bose–Einstein condensation of microcavity polaritons has produced a stream of breakthrough results [54, 55] (see also *exciton polaritons and their condensates*). Microcavity exciton polaritons display quantum effects including entanglement [56] and polariton blockade [57, 58] and may serve as a platform for the implementation of qubits [59].

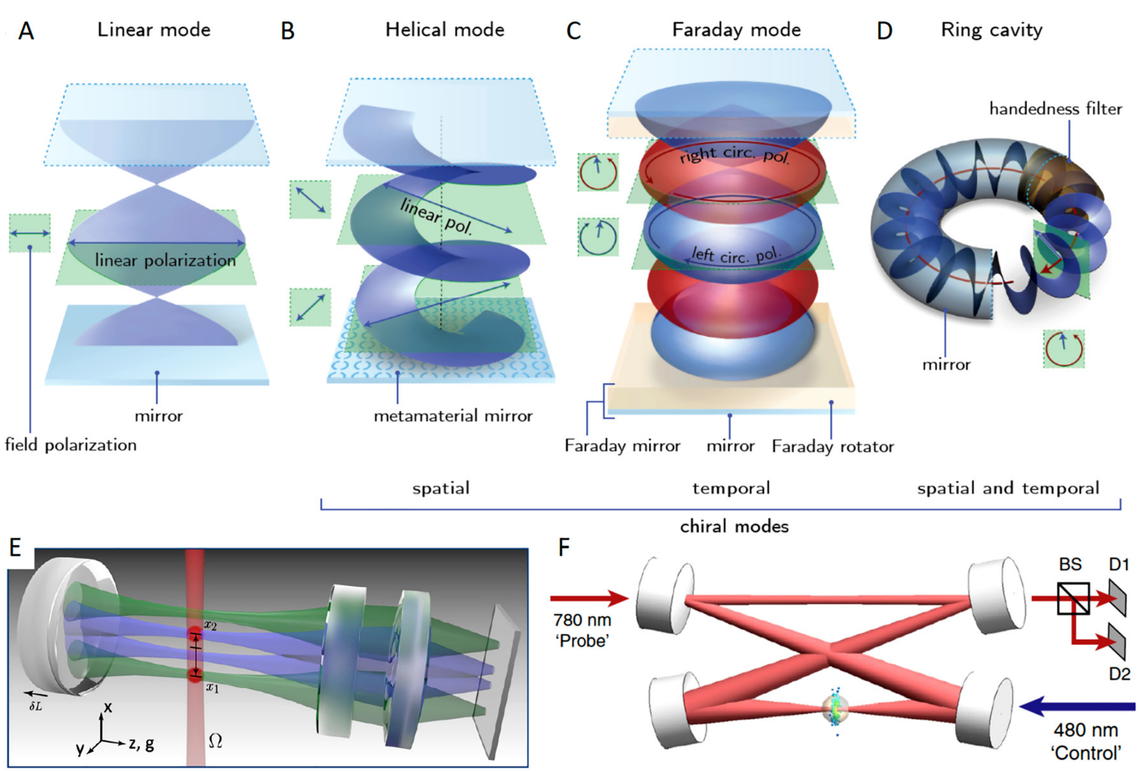

Box 2: Panorama of cavities and cavity modes. A common Fabry–Perot cavity (panel A) formed by two parallel mirrors supports linear modes and maintains time reversal symmetry. Cavities employing chiral metasurfaces support helical modes (panel B). A possible realization of time reversal symmetry breaking is offered by the use of Faraday mirrors in panel (panel C). Ring mode cavities (panel D) sustain running waves of a chosen circular polarization and break time reversal symmetry by means of a handedness filter realizable with a combination of a Faraday rotator and polarization optics. Advanced cavities are well suited for the exploration of the physics of spin vortices and skyrmion spin textures in exciton polariton condensates originating from the optical spin Hall effect [42, 43]. Panels A–D from a study by Hubener et al. [44]. Panel E is a multimode cavity quantum electrodynamics (QED) enabling local light–matter coupling. The schematic displays two ^{87}Rb Bose–Einstein condensates trapped at locations x_1 and x_2 on opposite sides of the cavity center [45]. Panel F is the schematic of a strongly interacting *polaritonic quantum dot* formed by 150 Rydberg-dressed Rubidium atoms in a single-mode optical resonator [46]. BS, beamsplitter; D1 and D2, single-photon detectors.

Channel polaritons are supported by materials and structures with a straight channel cut in polaritonic medium [60]. Channel polaritons were utilized for the implementation of waveguide components including interferometers and ring resonators [61]. Polaritons guided along the nanoslit are predicted to form *hybrid polaritons,* giving rise to both bonding and antibonding modes [62].

Charge transfer polaritons. The formation of plasmon polaritons in graphene or semiconductors relies on the high carrier density that can be introduced by electrostatic gating [63, 64], ferroelectric polarization [65], chemical doping [66], or photoexcitation [67]. Alternatively, the requisite carrier density can be introduced by charge transfer across the interface between proximal materials with dissimilar work functions. Such charge transfer plasmon polaritons have been demonstrated for graphene residing on another van der Waals material $RuCl_3$ [68]. Experiments on metallic nanoparticles show that charge transmitted between the pair of nanoparticles through a conducting pathway leads to a characteristic plasmonic response [69] termed *charge transfer plasmons*. Interlayer exciton in transition metal dichalcogenide (TMDC) heterostructures (e.g., $MoSe_2/WSe_2$) also involves charge transfer from one layer to another; the relevant microcavity polaritons [70] are classified as *charge transfer exciton polaritons*.

Charged polariton. Charged polaritons posess a nonvanishing electric charge. This interesting concept was introduced in the context of the cavity exciton polaritons in GaAs/AlAs quantum wells that also hosted two-dimensional electron gas with the density n_e. Spectroscopic experiments in a study by Forg et al. [71] have identified several distinct properties of charged exciton polaritons, including the scaling of the coupling strength analogous to the properties of atomic QED system [72]. The effective mass of charged polaritons exceeds the band mass of a GaAs quantum well by a factor of 200. Tiene et al. [73] have theoretically demonstrated the unique utility of charged microcavity polaritons for exploring the physics of electron–hole systems with charge imbalance, which are difficult to access with alternative experimental methods. They demonstrated how the Fermi sea of excess charges modifies both the exciton properties and the dielectric constant of the cavity medium, which in turn affects the photon component of the many-body polariton ground state (Figure 2). See also the closely related entries of *Fermi-edge exciton polaritons* and *trion polaritons*.

Cherenkov polaritons. In the Cherenkov effect [74], a charged particle moving with a velocity faster than the phase velocity of light in the medium radiates light. The emitted radiation forms a cone with a half angle determined by the ratio of the two velocities. Genevet et al. [75] demonstrated that by creating a running wave of polarization along a one-dimensional metallic nanostructure consisting of subwavelength-spaced rotated apertures that propagates faster than the surface plasmon polariton phase velocity, one can generate surface plasmon wakes that serve as a two-dimensional analog of Cherenkov radiation. The Cherenkov physics is also relevant to the properties of phonon polaritons [76, 77]. Infrared nanoimaging experiments reveal Cherenkov phonon polariton wakes emitted by superluminal one-dimensional plasmon polaritons in a silver nanowire on the surface of hexagonal boron nitride [78]. See also *Exciton polariton X-waves* on superluminal properties in the system of exciton polaritons.

Cooper pairs polaritons (in QMs and cold fermionic cavity systems). *Cooper pair plasmon polaritons* emerge in superconductors. The matter component of these polaritons is associated with the superfluid density (from a study by Basov et al. [1]). The dispersion of Cooper pairs plasmon polaritons in layered cuprate high-Tc superconductors has been investigated theoretically [13, 79] but is yet to be explored in experiments. Recently, the formalism of the Bardeen Cooper and Schrieffer theory of superconductivity has been applied to describe the quasiparticle excitations of a cold fermion system coupled to a cavity. Depending on the excitation density and atomic interaction, the excited atoms and holes and in the Fermi sea may form bound Cooper pairs strongly coupled with cavity photons. This latter kind of polaritons were also termed Cooper pair polaritons [80].

Dark polaritons in QMs: polaritons are characterized by a wavevector that lies beyond the light line. The lower branches of polaritons in many/most QM systems are dark by this criterion and do not couple to free space photons because of the notorious "momentum mismatch" problem (Box 1 F, H, Figure 1). Light excition of dark polaritons can be mediated by nanoscale defects such as a protrusions, divots, or cracks, exploiting the high spatial frequencies inherent to these deeply subwavelength objects. Better controlled strategies can also provide the missing momentum needed for coupling to dark polartons [81]. These include prism and grating coupling, and the use of plasmonic optical nanoantennas [82–89]. Notably, sharp scan probe tips can act as such antennas [90–95], allowing polaritonic waves to be launched and visualized. Scanning probe antenna-based nano-optics has emerged as an indespensible research tool enabling spectroscopy and visualization of polaritons in QMs [1, 88, 96].

Dark-state polaritons in atomic ensembles: typically, this refers to polaritons in atomic ensembles that propagate in the

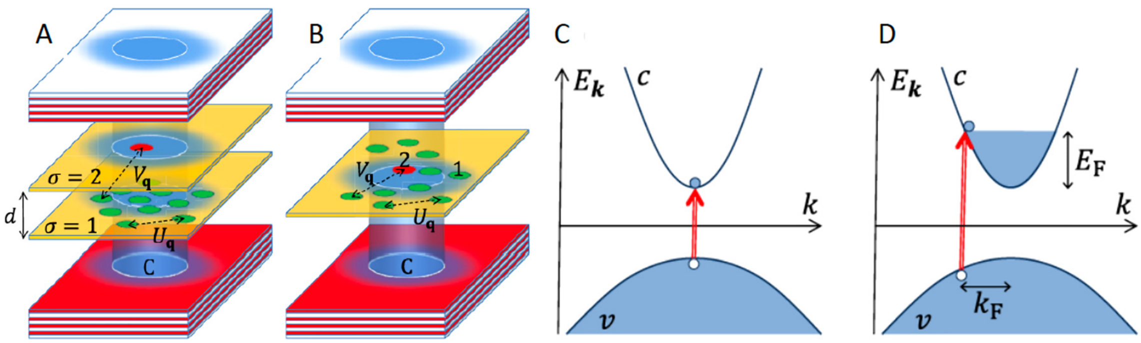

Figure 2: Charged exciton polaritons.
Panel A: two quantum wells, labeled with the indicies $\sigma = 1, 2$ and separated by a distance d, form an electron–hole bilayer in the extremely imbalanced limit. The minority species belongs to the $\sigma = 2$ layer, while the majority species at $\sigma = 1$ forms an interacting Fermi sea. U_q and V_q are, respectively, intraspecies and interspecies Coulomb interactions. The bilayer is located inside a planar cavity that confines the cavity photon mode C. The (blue) shaded area represents the finite-size external laser pump spot. Panel B: the same setup in a single quantum well geometry. Here, the majority $\sigma = 1$ and minority $\sigma = 2$ species belong to the same well. Panels C and D: the particle–hole excitation process via a photon without and with Fermi sea, respectively. All photon-mediated transitions are approximately vertical in a cavity. Adapted from a study by Tiene et al. [73].

regime of electromagnetically induced transparency (EIT) [97–100]. The darkness arises from the photon mixing strongly with a collective atomic excitation, resulting in a state with only a minute photonic component. See also *EIT polaritons* below. In ordered atomic arrays, dark (also often referred to as subradiant) states emerge due to interference in photon emission and absorption. At the single photon level, these darks states are collective spin excitations with a wave vector that lies beyond the light line, preventing the coupling with radiation modes (exactly the same phenomenon of "momentum mismatch" described above for QMs) [101–104]. Polaritons arising in atomic lattices have applications in quantum information storage and processing [103].

Demons: or density modes were introduced by David Pines [105], an early protagonist of plasmons research. *Demons* are particularly relevant to the response of the Dirac fluid in graphene in hydrodynamic regime [106] and adiabatic plasmon amplification [107].

Dirac plasmon polaritons are formed by hybrids of infrared photons with Dirac electrons in graphene [63, 64, 108, 109]. Direct nanoimaging experiments uncovered extraordinarily long propagation lengths of highly confined Dirac polaritons and have established fundamental limits underlying their decoherence and losses [110].

Dyakonov surface polaritons: the surface modes that propagate along the interface between isotropic and uniaxial materials is known as Dyakonov surface polaritons [111–113]. A special case of Dyakonov polaritons is realized in anisotropic crystals of layered van der Waals materials. One example is that of the *hyperbolic surface phonon polaritons* propagating along the edges of slabs prepared from hexagonal boron nitride [114–116].

Edge magneto plasmons. Two-dimensional (2D) electron gas subjected to the magnetic field normal to the plane of the 2D conductors reveals two distinct field-dependent resonances: the cyclotron resonance mode with frequency increasing with the magnetic field and another mode that redshifts with the applied field. The latter mode has been linked to the edge plasmons of the charged sheet and can be viewed as the 2D analog of surface plasmons in three-dimensional (3D) systems [117]. Specifically, edge magneto plasmons can propagate along the physical boundary of the 2D conductors [118, 119]. Edge magneto plasmons constitute a spectacular manifestation of the dynamical Hall effect. Edge magneto plasmons are chiral. Their chirality is a direct implication of the applied Lorentz force [120]. Graphene reveals rich plasmonic phenomena in the presence of magnetic fields [121–125].

Edge plasmon polaritons: one-dimensional plasmonic modes propagating along the physical boundaries of two-dimensional materials (Figure 3) is called edge plasmon polaritons. They reveal an approximately 10% shorter wavelength compared to the interior of the plasmonic medium [128]. Qualitatively, the shorter wavelength can be ascribed to the effective reduction of the Drude weight since free carriers exist only on one side of the physical boundary. *Dyakonov hyperbolic phonon polaritons* are a lattice analog of edge plasmon polaritons. Berini reported on an in-depth numerical analysis of edge and corner plasmon polariton modes in thin conducting slabs [129]. *Whispering-galley polaritons* is a special example of an edge polaritons that loops around the ridge of polartonic medium [130] or along the circumference of nanoholes [131, 132].

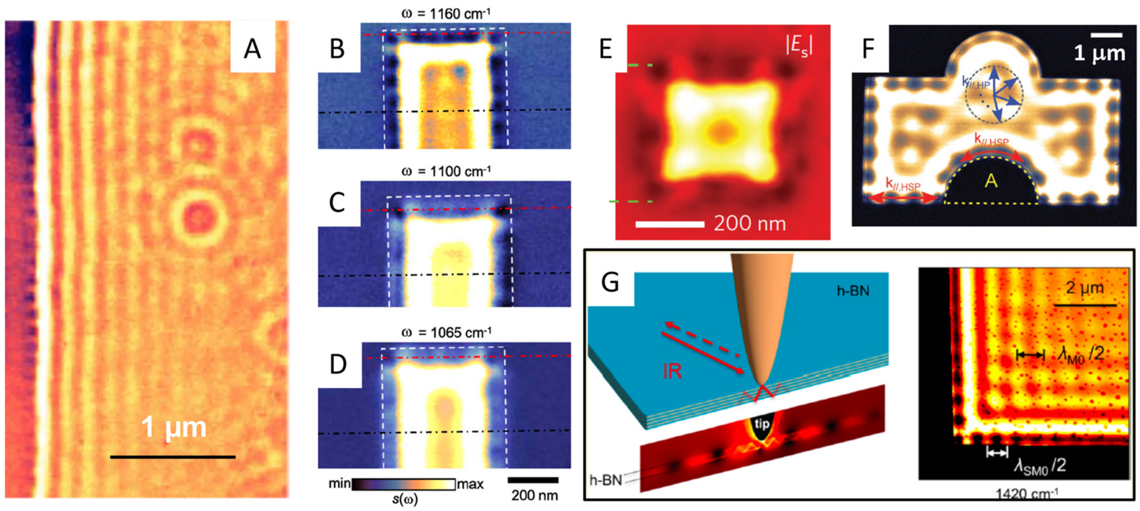

Figure 3: Interior and edge polaritons in van der Waals quantum materials.
Panel A: charge transfer plasmon polaritons at the interface of graphene and a-RuCl3 visualized by means of nanoinfrared methods ($\omega = 898\ \mathrm{cm}^{-1}$, $T = 60$ K). Three types of plasmonic fringes are observed: (i) edge plasmon polaritons (dark spots at along the physical boundary of graphene crystal), (ii) interior plasmon polaritons (oscillating wave pattern emanating from the boundary of graphene on the left), and (iii) defect-launched plasmon polaritons forming circular patterns in the interior of the sample. Adapted from a study by Rizzo et al. [68]. Panels B–D: nano-IR imaging of edge plasmons on graphene nanoribbons. White dashed lines mark the boundaries of the crosscut GNR. Adapted from a study by Fei et al. [126]. Panel E: nanoinfrared image of edge plasmons in a square sample of graphene. Adapted from a study by Nikitin et al. [128]. Panels F: nanoinfrared images of edge phonon polaritons in the 25-nm-thick slab of hBN. Adapted from a study by Dai et al. [114]. Panel G: edge and interior phonon polaritons in a 40-nm-thick slab of hBN [127].

EIT in nanoplasmonic structures [133, 134], EIT with plasmon polaritons in graphene [135, 136] and EIT with exciton polaritons in microcavities [137].

EIT polaritons propagate in atomic systems under conditions of EIT. A remarkable aspect of EIT polaritons is that they can be slowed down to 10s of meters per second [176] or even brought to a standstill [177, 178]. EIT polaritons can be dark (decoupled from radiation, more “atom-like”) or bright (coupled to radiation, more “photon-like”). The darkness/brightness of the polaritons is controlled by an external laser beam. EIT polaritons can be strongly interacting, if coupled to Rydberg states (see *Rydberg polaritons* below). The EIT phenomenon is also observed in materials and nanostructures. Examples include:

ENZ polaritons: epsilon-near-zero or ENZ polaritons are equivalent to *Berreman polaritons* above.

Exciton polaritons and their condensates. Exciton polaritons are bosonic quasiparticles originating from photons hybridized with hydrogen-like bound electron–hole pairs. Semiconductor microcavities (Box 1 and Figure 4A) offer an outstanding platform for the investigation of exciton polaritons and the attendant strong light–matter coupling, provided a high-quality microcavity is nearly resonant with an excitonic transition. Trapped photons may be emitted and reabsorbed multiple times before being lost to dissipation or cavity leakage. Absorption and re-emission of photons in the cavity give rise to light–matter mixed eigenstates [138]. When sufficiently long-lived, exciton polaritons may form coherent quantum states [139–145]. Bose–Einstein condensates (BECs) of exciton polaritons are appealing quantum liquids in part because their coherent state is created and controlled by light [146–148]. The binding energies of excitons in organic molecules [149], TMDCs, and lead halide perovskites can be as high as 0.75 eV [150–158]; these extraordinary high binding energies underlie the theoretical predictions of condensation and superfluidity at T = 300 K [159–161]. BECs of exciton polaritons were predicted to form spatially and temporarily ordered states: time crystals [162]. Exciton polariton condensates may also enable energy-efficient lasers [163].

Exciton polariton X-waves: wavepackets of exciton polaritons that sustain their shape without spreading, even in the linear regime. In a study by Gianfrate et al. [164]. Self-generation of an X-wave out of a Gaussian excitation spot is obtained via a weakly nonlinear asymmetric process with respect to two directions of the nonparabolic polariton dispersion. Notably, X-waves were found to propage with supluminal peak speed with respect to the group velocity of the polaritonic system.

Fermi edge exciton polaritons [165, 166] are observed in microcavities where the active semiconductor is

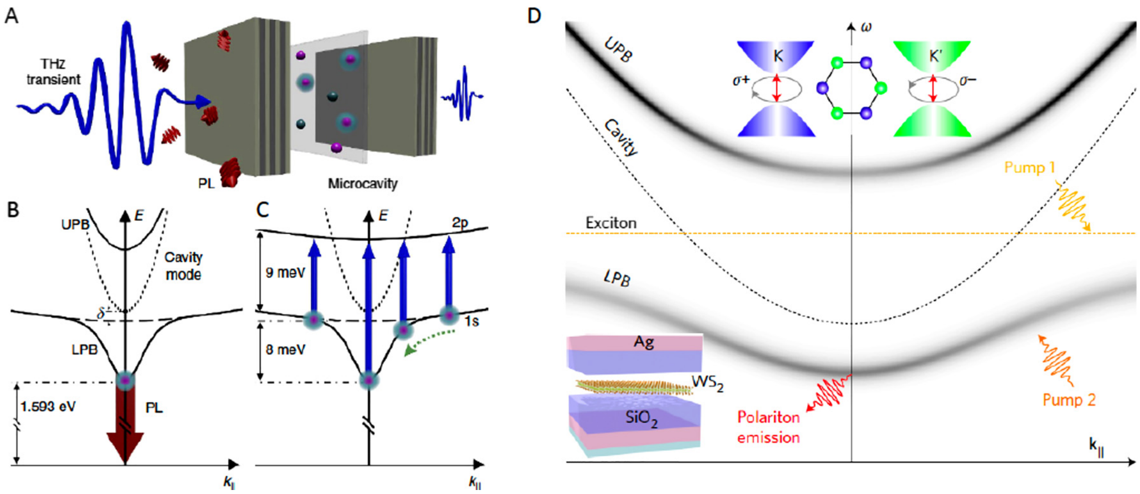

Figure 4: Cavity exciton polaritons.
Panel A: polaritons (pink spheres with blue halo) emerge from strong coupling between the excitonic resonance in a quantum well (transparent sheet) and the photonic mode of a GaAs/AlGaAs microcavity. THz probing (blue curve) maps out the matter component of the polaritons, while photoluminesce (PL, red arrows) leaking through a Bragg mirror reveals the photonic component. Panel B: normal-mode splitting. The heavy hole 1*s* exciton resonance (dashed curve) and the photonic mode (dotted curve) are replaced by the upper polariton branch and lower polariton branch (UPB and LPB, respectively; solid curves). PL (thick red arrow) originates from the radiative decay of polaritons at small in-plane momenta $k_{||}$. Panel C: THz absorption probes hydrogen-like intraexcitonic transitions. While the 1*s* state is spectrally shifted by strong light–matter coupling, the optically dark 2*p* exciton is not affected by the cavity. The resulting momentum dependence of the THz transition energy allows us to map out the momentum distribution of the polaritons as they relax toward $k_{||} = 0$ (green dotted arrow). From a study by Ménard et al. [174]. Panel D: schematic of the valley exciton polariton phenomena. The solid (gray) curves indicate LPB and UPB. The bare cavity and the exciton dispersion are shown by the black and orange dashed curves, respectively. Pump 1 is used to excite directly the exciton reservoir, whereas pump 2 excites the lower polariton branch at specific $k_{||}$ and ω. The emission is collected at smaller angles. The top inset shows the valley polarization phenomena in 2D transition metal dichalcogenide (TMDC) semiconductors caused by the broken inversion symmetry. In these materials, the *K* and *K′* points correspond to the band edges separated in momentum space but energetically degenerate. The bottom inset is a schematic of the microcavity structure with silver and a SiO_2 cavity layer embedded with prototypical TMDC materials WS_2. From a study by Sun et al. [175].

heavily doped to form the Fermi edge. Fermi edge exciton polaritons are formed of electron hole pair excitations involving electron and hole states with in-plane wave vectors around the Fermi edge: $k_{IIe} = k_{IIh} \sim k_F$, where k_F is the Fermi wavevector. In some literature, this latter form of polaritonic states are referred to Mahan exciton polaritons [167], recognizing a prediction of excitonic bound states in doped semiconductors beyond the critical density of the insulator to metal transition states by Mahan [168, 169]. See also *Quantum Hall polaritons* below.

Floquet polaritons. The concept of Floquet engineering refers to the control of a system using a time periodic optical field and is being broadly applied in atomic physics, as well as in the field of QMs [170]. The notion of Floquet polaritons pertains to polaritons in a system of Floquet-engineered atomic states [171] or electronic states in solids [172]. The concept of Floquet engineering by time period optical fields has been extended to coherent phonons in QMs [173]. *Chiral Floquet polaritons* are predicted [44] to form in chiral cavities, in which fundamental matter symmetries are broken (Box 2).

Frenkel exciton polaritons. The matter constituent of these polaritons originates from Frenkel excitons characterized by the Bohr radii of the same order as the size of the unit cell. Frenkel exciton polaritons are common in organic semiconductors [179]. The high exciton binding energy (~eV) and large oscillator strength may lead to room temperature exciton polariton condensates [180–182].

Fuchs–Kliewer interface polaritons: phonon polaritons occurring at surfaces and interfaces [183] with the matter part are originating from Fuchs–Kliewer surface phonons [184]. Huber et al. [185] employed nanoinfrared methods to visualize propagating Fuchs–Kliewer surface phonon polaritons in SiC. Surface phonon polaritons are observed in insulating and semiconducting materials including hBN [97, 98], SiC [186–189], GaAs [190], and many others.

Helical plasmon polaritons: were predicted to form in topologically nontrivial Weyl semimetals [191]. Plasmon polariton dispersion may enable the detection of a chiral anomaly: a charge imbalance between the Weyl nodes in the presence of electric and magnetic fields [192]. The Fermi surface of Weyl semimental features open disjoint segments – the Fermi arcs – associated with the topolical surface states. The resulting *Fermi arc plasmon polaritons* are predicted to be chiral and to reveal unidirectional propagation [193]. Helical plasmon terminology was also applied to describe one-dimensional plasmon polaritons associated with the helical state in domain walls of topologically nontrivial conductors including anomalous quantum Hall systems [194]. Helicity dependence of plasmon polaritons is discussed in the context of unidirectional propagation in plasmonic metastructures controlled by the circular polarization of light [195, 196].

Hopfield polaritons: a bold theoretical concept of light–matter hybridization proposed by John Hopfield in his doctoral thesis back in 1958 (in a study by Hopfield [197]). Hopfield also coauthored the first experimental paper on polaritons devoted to the study of phonon polariton dispersion in GaP by means of Raman scattering [198]. Other early contributions to the theory of polaritons (short of introducing this term) were made by Fano [199], Huang [200], and Tolpygo [201].

Hybrid polaritons. Different types of polaritons hosted by the same material are prone to hybridization [202]. For example, *intersubband polaritons* and *phonon polaritons* hybridize in semiconductor quantum wells [203–205]. Hybridization can also occur in multilayered structures. In all-dielectric layered structures, phonon polaritons associated with the neighboring layers couple to form hybrid modes [87, 206, 207]. Semiconductor heterostructures [208, 209] and especially van der Waals heterostructures offer a fertile platform for the implementation of hybrid polaritons [210, 211]. One such example (Figure 5B and C) is graphene surrounded by insulating layers of hexagonal boron nitride hBN or silicon dioxide. Plasmons associated with graphene layers hybridize with phonon polaritons in proximal SiO_2 or hBN layers to form *plasmon–phonon polaritons* [63, 64, 212, 213]. Hybrid polaritons at the interface of graphene with high-T_c superconductors were proposed as a tool to probe Anderson–Higgs electrodynamics [214]. Hybrid polariton at the interface of graphene with a charge density wave materials were theoretically proposed to “melt” the density wave order [215]. Hybrid modes produced by plasmons in graphene and molecular vibrations of absorbates on the graphene surface may enable high-selectivity sensing mechanisms [216, 217]. A special case of hybrid modes is *hybrid longitudinal–transverse phonon polaritons* [218]. Polaritonic heterostructures with phase change materials enable persistent switching of polaritonic response under thermal and optical stimuli [219].

Hyperbolic polaritons. Anisotropic media are predicted to support an interesting class of polaritonic light–matter modes referred to as “hyperbolic” because their isofrequency surface is a hyperboloid [213, 220–227]. These modes exist over a range of frequencies where the in-plane permittivity and the out-of-plane (*c*-axis) permittivity are of the opposite sign. Hyperbolic electrodynamics and hyperbolic polaritons can originate from a variety of physical processes including phonons [219, 223, 228–237] intersubband transitions in quantum wells [238–240] plasmons [220, 226, 241–244], excitons [245], and Cooper pairs (see *Cooper pair polaritons*). Hyperbolic polaritons dramatically enhance the local photonic density of states and are predicted to give rise to strong nonlinearities [246]. Hyperbolic polaritons enable canalization imaging [247] with image effectively transferred by high-momentum subdiffractional polaritonic rays from back to front surface of the polaritonic medium [248–251].

Image polaritons: virtual polariton modes produced by image charges at the interface of a polaritonic medium and a metal are called image polaritons. Lee et al. [252] have experimentally demonstrated low loss response of image polaritons at the interface of hBN separated with a thin spacer from a metallic substrate (Figure 5D).

Interband polaritons. The matter constituent of these polaritons originates from contributions of the optical response associated with transitions across the energy gap in the electronic spectrum of a material. These include transitions across the energy gap in semiconductors [253] and superconductors or transitions involving minibands/flat bands in moire superlattices of van der Waals materials [254–257] (see also *Moire polaritons*). The frequency dependence of $\sigma_2(\omega)x\omega$, where $\sigma_2(\omega)$ is the imaginary part of the complex conductivity, is informative for the analysis of interband polaritons [255, 258]. Spectra of $\sigma_2(\omega)x\omega$ reveal a series of steps separated by plateaus, with each step uncovering the energy scale associated with separate interband contributions. In the limit of $\omega \to 0$, the product $\sigma_2(\omega)x\omega$ quantifies the spectral weight of intraband processes to the plasmon polaritons. Interband effects play a central role in theoretical proposals for the implementation of population inversion [259], gain and *superluminal plasmon polaritons* [260].

Intersubband polaritons. Dini et al. [261, 262] reported the first experimental observation of the vacuum-field Rabi splitting of an intersubband transition inside a planar microcavity hosting two-dimensional electron gas. Nonlinearities associated with intesubband transitions in semiconductors can be dramatically enhanced by in hybrid structure with plasmonic metasurfaces [263] (see also *hybrid polaritons*).

Josephson plasmon polariton: an inherent attribute of strongly anisotropic layered superconductors is the

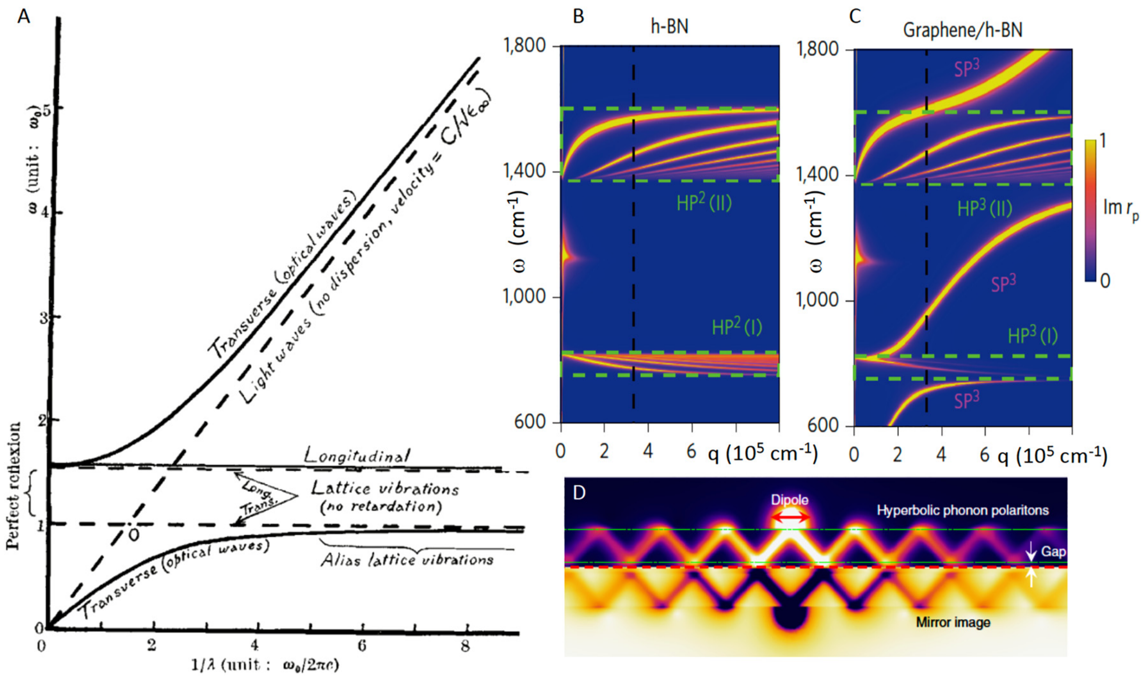

Figure 5: Phonon polaritons, hybrid plasmon–phonon polaritons, and image polaritons.
Panel A: dispersion of phonon polaritons in ionic crystals predicted by Huang (in a study by Sun et al. [175]). In the original publication, Huang did not use the term polariton. Panel B: calculated dispersion of the hyperbolic phonon polaritons in hBN (HP2). Panel C: calculated dispersion of the hyperbolic phonon polaritons in h-BN coupled to plasmon polaritons in the graphene layer and forming hyperbolic plasmon–phonon polaritons (HP3) and surface plasmon–phonon polaritons (SP3). Adapted from a study by Bezares et al. [212]. Panel D: concept of image polaritons at the interface of hBN and a metal. From a study by Yoo et al. [36].

Josephson plasmon polariton. The matter constituent of Josephson plasmon polaritons originates from interlayer Josephson plasmon in layered superconducting materials such as cuprates [79, 264]. Josephson plasmons are the electromagnetic signature of three-dimensional superconductivity in highly anisotropic layered high-T_c superconductors [265]. Josephson plasma waves can be parametrically amplified under illumination with pulsed THz fields [266], paving the way for active Josephson polaritonics.

Kane polaritons: surface plasmon polaritons formed with Kane quasiparticles is the Kane polaritons. Kane polaritons were recently observed in pump–probe experiments on narrow gap II–VI semiconductors [267].

Landau polaritons. The matter component of Landau polaritons originates from cyclotron resonances and transitions between quantized Landau levels relevant in low-dimensional electron gases subjected to high magnetic fields [268, 269]. See also *magneto plasmon polariton*.

Luttinger liquid polaritons: plasmon polaritons in one-dimensional conductors recently revealed by infrared nanoimaging of single-wall and multiple-wall carbon nanotubes [270]. Interacting electrons confined in one dimension are generally described by the Luttinger liquid formalism [271, 272]. Anomalous dependence of the plasmonic quality factor on gate voltage was interpreted in terms of plasmon–plasmon interaction in carbon nanotubes [273].

Magnon polaritons. The matter constituent of these polaritons originate from antiferromagnetic [274, 275] and ferromagnetic resonances [15]. In weak magnetic fields, *surface magnon polaritons* are predicted to acquire nonreciprocal properties. Macedo and Camley [276] analyzed the propagation of surface magnon polaritons in anisotropic antiferromagnets. Sloan et al. [277] predicted that surface magnon polaritons will strongly enhance the spin relaxation of quantum emitters in the proximity of antiferromagnetic materials such as MnF_2 or FeF_2. Kruk et al. [278] developed artificial structures with hyperbolic magnetic response with principal components of the magnetic permeability tensor having the opposite signs. Magnetic materials also support *hybrid polaritons*, including hybrid *magnon–phonon polaritons* recently observed in $ErFeO_3$/$LiNbO_3$ multilayers [279].

Magneto plasmon polaritons: coupled modes of magneto plasmons and THz/infrared photons [280, 281]. Theoretically predicted unconventional properties of magneto polaritons in Weyl semimetals include hyperbolic dispersion and photonic stop bands [282]. The nanoinfrared imaging and visualization of magneto plasmon polaritons remains an unresolved experimental challenge. Once technical obstacles are circumvented, it may become possible to directly explore both the focusing and the nonreciprocity predicted for magneto plasmon polaritons [283]. Plasmonic system driven by intense a.c. field is predicted to reveal spontaneous symmetry breaking and nonlinear magnetism [284].

Microcavity polaritons: see cavity polaritons.

Moire polaritons. Atomic layers comprising van der Waals materials can be reassembled into heterostructures with nearly perfect interfaces [285–287]. A unique control knob specific to vdW systems is the twist angle θ between the adjacent layers. Varying θ forms moiré superlattices that can radically modify the electronic structure and attendant properties [288–302]. Plasmons, phonons, and excitons are all altered in moire superlattices prompting changes of the corresponding polaritons. G/hBN[cross-Ni-Moire]. Infrared nanoimaging data display rich real space patterns of polaritonis with selected examples of moire polaritons displayed in Figure 6. Morie design principle can be applied to epitaxially grown thin films on dielectric substrates [303]. Recent experiments on interlayer excitons in TMDC heterobilayers have revealed the trapping of these excitons on the moire potential landscape [304–307]. When placed in an optical cavity, such moire trapped excitons may form an exciton polariton lattice and serve as analog quantum simulators (QSs) (see *polaritonic lattices and quantum simulators*).

Molecular polaritons. Organic semiconductors and molecules embedded in optical (nano)cavities under strong and ultrastrong coupling promote the dynamical formation of molecular polaritons: hybrid energy eigenstates composed of entangled photonic, electronic, and vibrational degrees of freedom [34, 312, 313]. Molecular polaritons were demonstrated to enhance energy transfer [314] and DC conductivity [315]. Progress with nanostructures enabled a demonstration of the strong–light matter coupling with a single molecule embedded in a plasmonic cavity [316]. Molecular molaritons enable control of optical nonlinearities via manipulations of cavity characteristics [317]. Molecular polaritons can form *hybrid polaritons* by coupling to surface plasmons [318], for example. We remark that molecular polaritons are commonly referred to as *vibrational polaritons*.

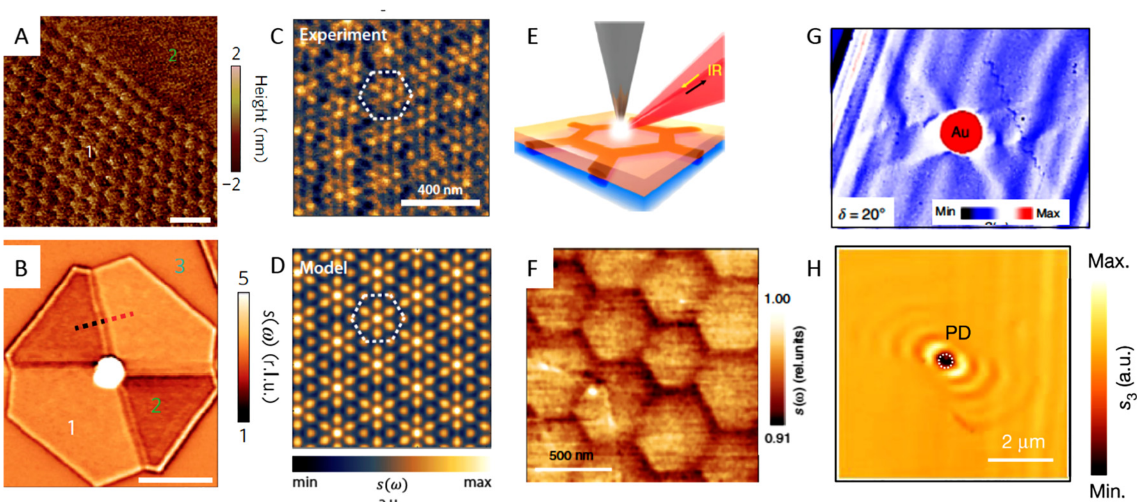

Figure 6: Moire polaritons and topological phonon polaritons in twisted van der Waals materials.
Panel A: atomic force friction image of the graphene/hBN structure at the boundary between the moiré-superlattice and plain graphene (marked in Panel B). Moire reconstruction leads to a periodic pattern with the periodicity of 14 nm. Scale bar 1 µm. Panel B: nanoinfrared image of the graphene/hBN structure. Darker contrast occurs in the moire region. The analysis of plasmon polariton fringes along the boundary between moire superlattice and plain graphene allows one to reconstruct the gross feature of the altered electronic structure in the moire superlattice region. Adapted from a study by Ni et al. [255]. Panel C: nanoinfrared image of plasmon polaritons interference patterns in a moiré superlattice formed by twisted layers of graphene. The dashed hexagons represent the boundaries of a single unit cell. From a study by Sunku et al. [308]. Panel D: plasmon polariton superposition model, which accounts for the gross features of the image in C. Panel E: schematic of the nano-IR imaging showing an AFM tip illuminated by a focused IR beam. Panel F: nanoinfrared image of moire superlattice pattern in hBN. The contrast is formed by the shift and broadening of the phonon polariton resonance. Adapted from a study by Ni et al. [309]. Panel G: nanoinfrared image of phonon polaritons in a twisted structure of MoO_3 slabs rotated by θ = 20°, revealing complex wavefront geometry. adapted from a study by Chen et al. [310]. Panel H: topological phonon polaritons in twisted MoO_3 slabs rotated by $\theta = 77°$. From a study by Hu et al. [311].

Mott polaritons (QED): nonequilibrium driven states in an array of circuit QED cavities or optical resonators [319, 320] is the Mott polaritons. See also *polaritonic lattices*.

Mott polaritons (QM) were also introduced in context of the resonant coupling between strongly correlated electrons in solid Mott insulators integrated in a single-mode cavity [321].

Phonon polaritons: is a collective excitation comprised (infrared) light coupled with a polar lattice vibration. Like other polaritons, phonon polaritons can be understood in terms of an anticrossing of the dispersion curves of light and matter constituents (Figure 5). Early observations of phonon polaritons (see *Hopfield polaritons*) in bulk crystals and films were made using a variety of spectroscopic methods [322, 323]. More recent work [324] has focused on the generation, detection, and on picosecond polaritons dynamics [325–329]. By matching the phonon polariton velocity in $LiNbO_3$ crystal to the group velocity of the *fs* punp pulse Yeh et al. [330] have been able to generate intense THz fields of the order of 10 μJ energy. Advanced nanoimaging/spectroscopy methods [331–333] were employed for the real-space visualization of phonon polariton standing ways. Phonon polaritons play a major role in nanoscale thermal transport at nanoscale and mesoscale [86, 334–339]. Phonon polaritons in the anisotropic oxide material MoO_3 reveal both elliptical and hyperbolic dispersions [339–341]. The dispersion and propagation of phonon polaritons can be controlled by nanostructuring [342] and twist-angle (moire) engineering (Figure 6). The recent discovery of parametric phonon amplification in SiC paves the way for the exploration of nonlinear and active phonon polariton phenomena [343]. *Surface phonon polaritons* (see also *Fuchs–Kliewer* interface polaritons) reveal a dispersion branch located between longitudinal and transverse vibrational modes (see *hybrid polaritons*). Dai et al. [344] detected surface phonon polaritons in monolayers of hBN.

Plasmon polaritons: probably the most thoroughly studied class of polaritons. A surface plasmon polariton is a transverse magnetic (TM)-polarized optical surface wave that, for example, propagates along a flat metal–dielectric interface, typically at visible or infrared wavelengths [345–347]. Plasmon polaritons have rich implications for technology [348–351]. Nonlinear [352–354] and quantum [355–359] properties of plasmonic structures are in the vanguard of current research. Plasmon polaritons can be controlled at femto-second timescales [67, 267, 360–363] enabling access to novel physics and applications [364, 365]. Plasmonic waveguides have been incorporated with light-emitting materials, paving the way for integrated plasmonic and photonic structures [366]. Plasmon polaritons have been harnessed to implement high-quality factors such as whispering gallery microcavities [367]. In parallel, many research groups are searching for new plasmonic media with the properties optimized for different classes of plasmonic effects [368–371]. Van der Waals materials, and especially graphene, are emerging as outstanding plasmonic media in light of their inherent tunability with different stimuli (see *Dirac plasmons*). *Acoustic plasmon polaritons* are a special example of *hybrid polaritons* whose frequency-momentum $\omega(q)$ dispersion is predicted to be linear [372–376]. Acoustic plasmon plaritons have been demonstrated [377–379] in structures, where graphene resides in close proximity to metallic surfaces. *Spoof surface plasmons polaritons* were introduced describe plasmon polaritons on the surface of artificial metallic structures and metamaterials [380]. *Airy surface plasmon polaritons* are the surface counterparts of nondiffracting airy waves [381] and have been demonstrated by direct nanoimaging [382]. *Chiral plasmon polaritons* [383] were predicted to occur in twisted bilayer graphene [384] (Figure 7).

Plexcitons are a specific example of hybrid polaritons. The matter constituent of plexcitons originates from plasmon exciton coupled modes [386–392] Historically, plexciton studies have focused primarily on localized states [387, 393]. Propagating plexciton states also exist and offer potential for compact quantum information carriers as well as opportunities for mediating emitter–emitter coupling [394–396]. Composite structures and multilayers can feature plexcitons. An interesting recent example of plexciton study has been conducted in the setting of scanning probe nano-optical imaging and spectroscopy (Figure 8). This work by May et al. [398], along with a study by Groß et al. [397], implemented the scanning optical cavities formed between a nano-optical antenna and the substrate. The authors investigated CdSe/ZnS quantum dots using this scanning cavity approach and observed plexitonic Rabi splitting of 163 meV.

Polaritons parametric amplification, gain, and lasing have been demonstrated for exciton polaritons in microcavities [52, 399–401]. Resonant coupling between photons and excitons in microcavities can efficiently generate significant single-pass optical gains [399]. Polaritonic lasing has been implemented and analyzed in different material systems hosting *plasmon polartions* and *exciton polaritons* [402]. Amplification of *demons* [107] has been predicted as well but is yet to be experimentally demonstrated.

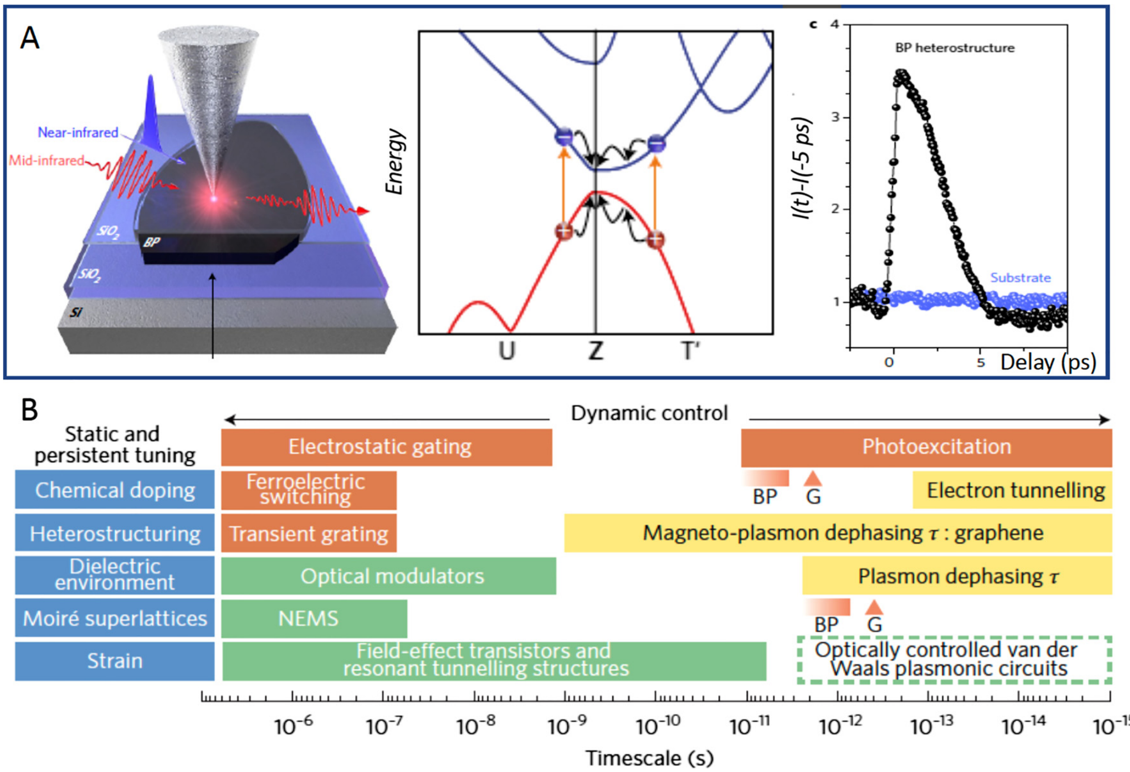

Figure 7: Ultrafast plasmonic effects in van der Waals materials.
Panel A: nanoinfrared spectroscopy and imaging of switchable plasmon polaritons in black phosphorous (bP) semiconductor. Left: experimental schematics. Middle: band structure of bP. Orange arrows indicate electron–hole pairs excited by a near-infrared pulse centered at a wavelength of 1560 nm. The curved black arrows indicate carrier cooling toward the band extrema. Right: Ultrafast pump–probe dynamics of the scattered near-field intensity normalized to the signal at the negative delay time (equilibrium). The SiO_2 substrate (blue points) shows no dynamics, whereas the SiO_2/bP/SiO_2 heterostructure (black points) features a strong pump–probe signal. Adapted from a study by Eisele et al. [362]. Panel B: methods for controlling plasmons in van der Waals materials and the corresponding timescales. Static and persistent tuning methods are displayed in the blue boxes; dynamical control methods are displayed in the orange ones. The yellow boxes show the dephasing times (τ) of plasmons and magneto plasmons in van der Waals materials along with characteristic timescales of electron tunneling in these systems. The green boxes represent timescales pertinent for various photonics technologies. The box with the dashed green outline indicates the desired timescales for future ultrafast plasmonic circuits. NEMS, nanoelectromechanical systems; G, graphene. Adapted from a study by Basov et al. [385].

Polaritonic chemistry: an emerging field focused on modifying pathways of chemical reactions in molecular systems coupled to photonic cavities [403–407].

Polaritonic circuits, devices, arrays, and systems. Both light and matter constituents of polaritons are amenable to controls with external stimuli [408]. The use of *exciton polaritons* as building blocks for future information processing such as spin switches [409], spin memory [410], transistors [411], logic gates [412], resonant tunneling diodes [413], routers [414], and lasers [415] has recently been demonstrated. The first polaritonic systems are also emerging and include QSs and networks for neuromorphic computers [416]. TMDC material WSe_2 integrated into microcavity devices acts as efficient light emitting device [417].

Polaritonic lattices, and QSs. A variety of experimental approaches have been utilized to implement one- and two-dimensional arrays of interacting polaritons. In the field of *microcavity exciton polaritons* gate arrays, spatially dependent optical potential as well as surface acoustic waves [418], have been utilized to generate arrays/lattices [419]. One-dimensional *exciton polariton* superlattices reveal weak lasing assigned to a novel type of a phase transition in this interacting system [420]. Arrays of evanescently coupled cavities hosting neutral atoms [421] have been proposed as QSs, where the photon blockade provided by the atom limits the occupancy of each cavity to one, allowing for the implementation of the Bose–Hubbard model. QSs require controllable quantum systems that efficiently simulate a Hamiltonian of interest, which may encode phases with a significant degree of entanglement and is not amenable to calculations by classical computer [422–427]. Lattices of *exciton polaritons* [422, 428–432] have emerged as a promising platform for QS, along with ultracold atoms [425, 433], trapped ions [434–436], and superconducting circuits

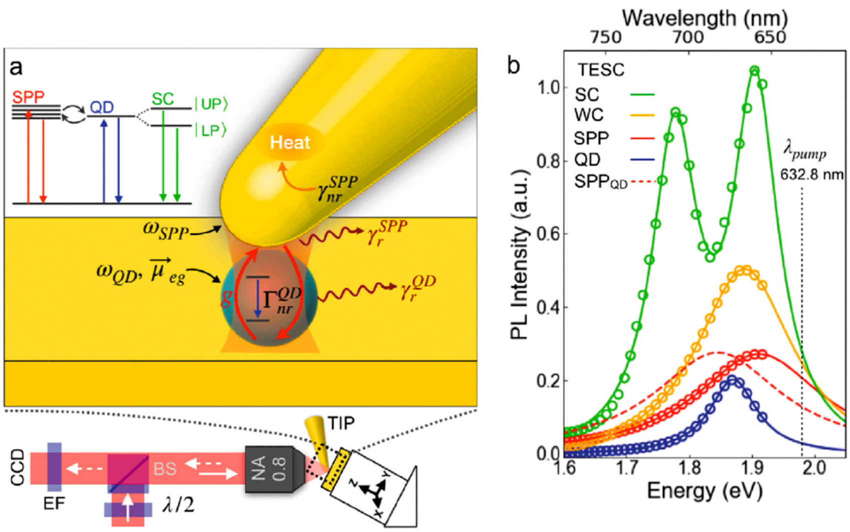

Figure 8: Tip-enhanced spectroscopy of plexcitons.
Panel A: the strongly confined $|E_z|$ field in a plasmonic nanogap cavity surrounding a single isolated CdSe/ZnS quantum dot (QD) and a tilted Au tip induce coupling between the plasmon and exciton. Panels B: Measured PL spectra for the QD, cavity plasmon polariton, weakly coupled system (WC) and strongly coupled states (SC) with coupling strength $g = 141$ meV. A Lorentzian lineshape representing the redshifted plasmon resonance in the presence of the QD is calculated from the fitted values (SPP_{QD}) [398].

[437, 438]. Moire superlattices of *plasmon polaritons* (Figure 6) present yet another example of polaritonic lattices. Moire superlattices were realized in graphene devices with nanostructured gate electrodes [439], as well as in moire superlattices of twisted graphene layers [308].

Polaritonic interference, refraction, collimation, front shaping, and waveguiding. All these common wave phenomena are relevant to polaritons (Figure 9). In van der Waals materials, domain wall boundaries can act a polaritonc reflectors [440–442], or conductors [443]. Zia and Brongersma [444] demonstrated Young's double-slit experiments with surface *plasmon polaritonss*. Beyond analogs of geometrical optics effects, polaritons offer at least two novel routes for image formation. First, *hyperbolic polaritons* enable canalization imaging [247], with images effectively transferred by high-momentum subdiffractional polaritonic rays from the back to the front surface of the polaritonic medium [248, 250, 311, 445] (Figure 9C). Second, polaritons are amenable to guiding and steering using methods of *transformation optics*. Polaritonic waveguides have been implemented over a broad range of frequencies from THz [446] and infrared regions to visible light. Peier et al. observed phonon–polariton tunneling across the airgap [447]. Advanced polaritonic launchers and metalenses (Figure 9D) are well suited for defining the trajectories of polaritonic surface "beams" [448, 449]. In highly nonlinear regime polaritons are predicted to display self-focusing effects and to form solitons [450].

Polariton–polariton interactions. The interaction of polaritons stems from their underlying matter constituents. In close analogy with other interacting systems, polariton–polariton interactions renormalize the dispersion and also prompt a blue shift of the emission energy as the polariton density increases [451, 452]. Polariton–polariton interaction

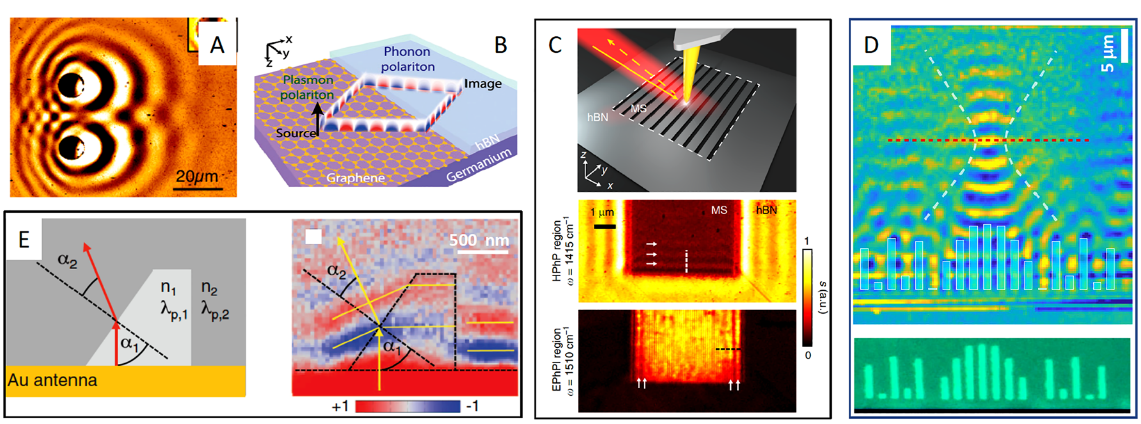

Figure 9: Infrared nanoimaging of polaritonic waves.
Panel A: nano-IR image of the interference pattern of surface *phonon polaritons* on a SiC launched by circular Au discs [331]. Panel B: prediction of in-plane negative refraction between *plasmon polaritons* in graphene and *phonon polaritons* in an hBN slab [455]. Panel C: nano-IR imaging of polariton evolution and canalization in an hBN metasurface [248]. Panel D: optical images of the laser-written metalense (bottom). Nano-IR image of revealing focusing of *phonon polaritons* at 1452 cm^{-1} [456]. Panel E: refraction of graphene *plasmon polaritons* at the prism formed by bilayer graphene [457].

effects have been recently demonstrated for *microcavity exciton polaritons* [453, 454]. See also *quantum Hall polaritons*.

Polaron polaritons. In TMDC monolayers, the itinerant electrons dynamically screen exciton to form new quasiparticle branches – the attractive and repulsive polaron – each with a renormalized mass and energy [458, 459]. *Microcavity polaritons* with the matter constituent linked to these polaron branches are referred to as polaron polaritons [458].

Quantum Hall polaritons are a product of coupling cavity photons to the cyclotron resonance excitations of electron liquids in high-mobility semiconductor quantum wells or graphene sheets [460, 461]. The edge channels of the quantum Hall effect offer a platform for probing interference and entanglement effects in the setting of a condensed matter system since the edge states propagation is ballistic, one-dimensional, and chiral. This platform enables experimental implementation of electron quantum optics [462–465] and may be suitable for the realization of flying qubits. In a parallel development, Smolka et al. [466]. investigated cavity *exciton polaritons* in the presence of high-mobility 2D electron gas subjected to external magnetic field and discovered novel correlated electron phases. Knuppel et al. [467] reported on strong *polariton–polariton interactions* in the fractional quantum Hall regime.

Rydberg polaritons (QED): photons dressed by highly excited atomic Rydberg states under conditions of electromagnetic induced transparency. These polaritons can either reside in a cavity or propagate throughout an atomic ensemble. In a cavity, Rydberg dressing bestows an atomic ensemble with the character of a two-level system: the excitation of a single Rydberg polariton prevents the creation of a second one, in the so-called “Rydberg blockade” regime. Under conditions of *electromagnetic induced transparency*, polaritons can propagate within an optically dense atomic cloud. These polaritons can then be made to interact with each other via Rydberg dressing: the first Rydberg polariton alters the transparency condition for the second one, preventing its propagation within a certain “blockade radius” [470–473]. Rydberg polaritons are appealing for quantum logic functionalities [474] and for realizing synthetic materials via many-body states of light [140, 171].

Rydberg polaritons (QM): a special example of *exciton polaritons* with matter constituent associated with strongly interacting Rydberg states of excitons [137]. Candidate systems include TMDC monolayers [475, 476] and cuprous oxide, where Rydberg states with principal quantum numbers of up to $n = 25$ are feasible [477].

Soliton polaritons. Propagating wavepackets in semiconductor micorcavities are referred to as soliton polaritons (Figure 10C). In quantum optics, topological soliton polaritons refer to composite objects made of fermions trapped in an optical soliton. The prototypical one-dimensional (1D) model of solitons posessing nontrivial topology is the model of Su–Schrieffer–Heeger (SSH) chains [478]. Variants of the SSH Hamiltonian have been emulated in the 1D lattices of *microcavity exciton polaritons* [479] and also in the system of quantum emitters coupled to a photonic waveguide [480]. Topological phases of polritons in cavity waveguides were analyzed in a study by Downing et al. [481].

Spin polaritons: this term was coined in the context of polariton microcavity diode lasers operating via injection of spin polarized currents [482].

Spin plasmon polaritons are relevant to the plasmonic response of spin-polarized electron gas [483]. Alternatively, spin–orbit interaction may lift the degeneracy between the spin states and give rise to transitions responsible for peculiar dispersion features of spin plasmon polaritons [484]. The surface plasmon of a helical electron liquid is predicted to carry spin and is also referred to as a spin plasmon polariton [485].

Transformation optics with polaritons. Transformation optics refers to a general principle for designing a complex electromagnetic medium with tailored properties by carefully crafting the spatial patterns of the local optical index [486, 487]. This general principle has been extended to

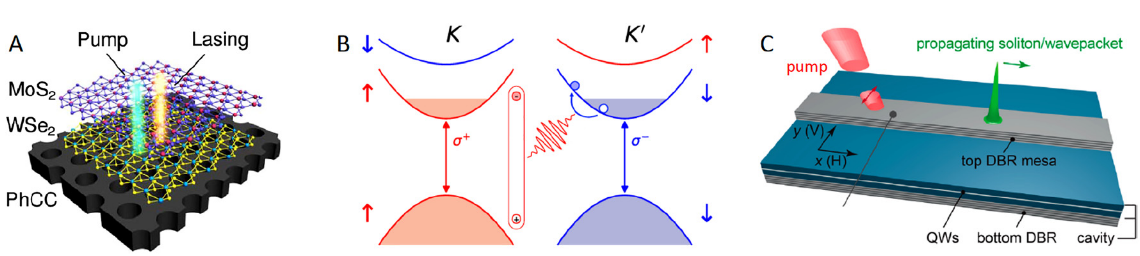

Figure 10: Panel A: schematic of MoS_2/WSe_2 heterobilayer nanolaser integrated in photonic crystal cavity [402]. Panel B: polaron–polaritons in TMDC semiconductors. Schematic to illustrate the conduction and valence band structure and optical selection rules of monolayer $MoSe_2$ close to the *K* and *K′* points. An exciton in the *K* valley interacts with conduction band electron–hole pairs in the Fermi sea of the *K′* valley to form an intervalley polaron. From a study by Bing Tan et al. [468]. Panel C: experimental setup for the exploration of propagating solitons in the system of microcavity exciton polaritons [469].

polaritons [488] and polartonic cavities [489], and specifically to *plasmon polaritons* in graphene [490]. Losses present the most significant experimental roadblock for practical transformational polaritonics. Recent advances with highly confined but low-loss plasmon polaritons [110] and phonon polaritons [223] fulfill important experimental preconditions for the realization of transformation optics ideas in polaritonic systems.

Tamm surface plasmon polaritons are associated with Tamm states at metallic surfaces [491]. Common surface *plasmon polaritons* are formed with a TM polarization at the boundary of metallic and dielectric surfaces and lie to the right of the light cone. Tamm polaritons are found with both TM and transverse electric polarizations, and their dispersion can be within the light cone [492, 493].

Trion polaritons. The matter constituent of these polaritons is formed by charged excitons or trions (see also *charged polaritons*). Trion polaritons are commonly found in the response of TMDC semiconductors [494, 495] and also in carbon nanotubes [496].

Tunneling plasmon polaritons were predicted [497] and observed [498] in an atomically thick tunable quantum tunneling devices consisting of two layers of graphene separated by 1 nm of h-BN. By applying a bias voltage between the graphene layers, one creates an electron gas coupled to a hole gas. Even though the total charge of the devices is zero, this system supports propagating graphene plasmons.

Valley polaritons. The matter constituent of these polaritons originates from valley polarized excitons in TMDC semiconductors (Figure 4B and *exciton polaritons*). The electronic structure of two-dimensional TMDC semiconductors endows this class of materials with the spin–valley degree of freedom that provides an optically accessible route for the control and manipulation of electron spin [499–501].

Vibrational polaritons: see molecular polaritons.

Wannier or *Wannier–Mott polaritons* borrow their matter part from Wannier excitons in semiconductors [502].

Waveguides and photonic crystals for polaritons. Waveguides and photonic crystals allow one to design and control the properties of photons, and thus of polaritons, both in quantum optics and QMs. In waveguide QED, different type of emitters (neutral atoms, quantum dots, color centers, superconducting qubits) are coupled to a

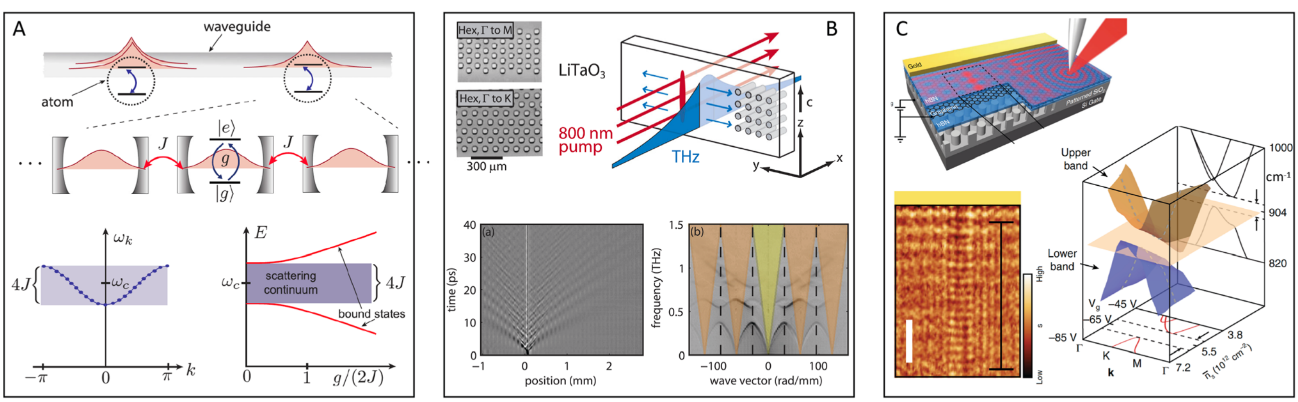

Figure 11: Polariton waveguide QED.
Panel A: emergence of bound atom–photon dressed states in 1D waveguides with finite bandwidth. The slow-light waveguide can be modeled as a large array of coupled optical resonators with nearest-neighbor coupling J. Lower left: band structure of the waveguide without atoms. Lower right: single-photon spectrum as a function of the atom–photon coupling g in the case of a single atom (with $\omega a = \omega c$) coupled to the waveguide, showing the emergence of bound states. Reproduced from a study by Calajo et al. [503]. Panel B: Photonic crystal for phonon polaritons in $LaTaO_3$. Top left: optical microscope images of the photonic crystal patterns. Top right: schematic of pump–probe experiments. Bottom left: space–time plot of THz waves generated directly inside a square photonic crystal. The edges of the image are the edges of the photonic crystal. Bottom right: dispersion diagram obtained from a 2D Fourier transform of the space–time plot in bottom left panel. The region highlighted in yellow represents the light cone. The regions highlighted in orange show the locations of the leaky modes. Adapted from a study by Ofori-Okai et al. [504]. Panel C: tunable and switchable photonic crystal for surface plasmon polaritons in graphene. Top: Schematic of a photonic crystal comprised of a graphene monolayer fully encapsulated by hexagonal boron nitride on top of an array of SiO_2 pillars. Pixelated gate insulator implemented in the form of nanopillars enables the local modulation of the carrier density and therefore of the plasmonic density of states. Bottom left: near-field nano-IR image of plasmonic standing waves for a structure in the top panel. Scale bar 400 nm. Bottom right: calculated plasmonic band structure as a function of wave vector k and average carrier density ns. A vertical cut parallel to the ω–k plane (back panel) generates the plasmonic band structure at fixed carrier density $n_s = 5.5 \times 10^{12}$ cm^2. The dashed lines mark the range of a complete plasmonic bandgap. A horizontal cut parallel to n_s–k plane (bottom panel) generates the plasmonic dispersion as a function of average carrier density ns and wave vector k, at laser frequency $\omega = 904$ cm^{-1}; a complete bandgap is evident for carrier density around $n_s = 5.5 \times 10^{12}$ cm^2.

one-dimensional (1D) optical channels [505], such as fibers [506, 507], photonic crystals [508, 509], and transmission lines [510, 511] (Box 1 and Figure 11A). Channel with a bandgap give rise to atom–photon bound states (i.e., polaritonic bound states), provided the atomic resonance frequency is close to the band edge. Beyond the band-edge, photons are bound to the atoms, forming localized polaritonic cavities that can be harnessed for realizing quantum simulation and quantum information processing (Box 1). If the coupling between photons and atoms is strong enough, bound states emerge even if the atomic resonance frequency lies inside the band (i.e., as a "bound states in the continuum") due to multiple scattering [503, 512]. In the field of QMs, photonic crystal structures were fabricated using common phonon–polariton oxide systems $LiTaO_3$ and $LiNbO_3$ (Figure 11B). Pump–probe experiments in Figure 11B revealed the key attributes of the dispersion control by these periodic structures. A significant deficiency of conventional photonic crystals is that they do not allow for dynamical dispersion engineering. Xiong et al. circumvented this limitation and demonstrated a broadly tunable two-dimensional photonic crystal for *surface plasmon polaritons* [cross-ref-xiond]. Infrared nanoimaging revealed the formation of a photonic bandgap and an artificial domain wall which supports highly confined one-dimensional plasmonic modes.

Zenneck–Sommerfeld waves and Norton waves: an early example of a guided electromagnetic wave at the interface of media with negative and positive dielectric function [513–515], the same condition that is required for the formation of polaritonic modes in THz, infrared, and optical frequencies. The original prediction of Zenneck–Sommerfeld waves pertained to the radiofrequency wave at the interface of air and the Earth. In this analysis, the surface of the Earth was regarded as a lossy dielectric. The concept of Zenneck–Sommerfeld waves and closely related Norton waves has been applied to a broad class of wave patterns on the surface of metallic [516–519] and dielectric materials [520].

Acknowlegements: Research at Columbia is supported as part of Programmable Quantum Materials, an Energy Frontier Research Center funded by the U.S. Department of Energy (DOE), Office of Science, Basic Energy Sciences (BES), under award DE-SC0019443. D.N.B. is Vannevar Bush Faculty Fellow ONR-VB: N00014-19-1-2630 and Moore Investigator in Quantum Materials #9455.
Author contribution: All the authors have accepted responsibility for the entire content of this submitted manuscript and approved submission.
Research funding: Research at Columbia is supported as part of Programmable Quantum Materials, an Energy Frontier Research Center funded by the U.S. Department of Energy (DOE), Office of Science, Basic Energy Sciences (BES), under award DE-SC0019443.
Conflict of interest statement: The authors declare no conflicts of interest regarding this article.

References

[1] D. N. Basov, M. M. Fogler, and F. J. Garcia de Abajo, "Polaritons in van der Waals materials," *Science*, vol. 354, p. 195, 2016.
[2] D. N. Basov, R. D. Averitt and D. Hsieh, "Towards properties on demand in quantum materials," *Nat. Mater.*, vol. 16, p. 1077, 2017.
[3] T. Low, A. Chaves, J. D. Caldwell, et al., "Polaritons in layered two-dimensional materials," *Nat. Mater.*, vol. 16, p. 182, 2017.
[4] D. E. Chang, J. S. Douglas, A. Gonzalez-Tudela, C.-L. Hung, and H. J. Kimble, "Colloquium: Quantum matter built from a nanoscopic lattices of atoms and photons," *Rev. Mod. Phys.*, vol. 90, p. 031002, 2018.
[5] A. A. Clerk, K. W. Lehnert, P. Bertet, J. R. Petta and Y. Nakamura, "Hybrid quantum systems with circuit quantum electrodynamics," *Nat. Phys.*, vol. 16, p. 257, 2020.
[6] I. Carusotto, A. A. Houck, P. Roushan, D. I. Schuster, and J. Simon, "Photonic materials in circuit quantum electrodynamics," *Nat. Phys.*, vol. 16, p. 268, 2020.
[7] M. Ruggenthaler, N. Tancogne-Dejean, J. Flick, H. Appel, and A. Rubio, "From a quantum-electrodynamical light–matter description to novel spectroscopies," *Nat. Rev. Chem.*, vol. 2, p. 0118, 2018.
[8] P. Forn-Díaz, L. Lamata, E. Rico, J. Kono, and E. Solano, "Ultrastrong coupling regimes of light–matter interaction," *Rev. Mod. Phys.*, vol. 91, p. 025005, 2019.
[9] A. Michael, J. L. Sentef, F. Künzel, and M. Eckstein, "Quantum to classical crossover of Floquet engineering in correlated quantum system,s" *Phys. Rev. Res.*, vol. 2, p. 033033, 2020.
[10] A. F. Kockum, A. Miranowicz, S. De Liberato, S. Savasta, and F. Nori, "Ultrastrong coupling between light and matter," *Nat. Rev. Phys.*, vol. 1, p. 19, 2019.
[11] R. Jestädt, M. Ruggenthaler, M. J. T. Oliveira, A. Rubio, and H. Appel "Light–matter interactions within the Ehrenfest–Maxwell–Pauli–Kohn–Sham framework: fundamentals, implementation, and nano-optical applications," *Adv. Phys.*, vol. 68, p. 225, 2020.
[12] Z. M. Raines, A. A. Allocca, M. Hafezi, and V. M. Galitski, "Cavity Higgs polaritons," *Phys. Rev. Res.*, vol. 2, p. 013143, 2020.
[13] Z. Sun, M. M. Fogler, D. N. Basov, and A. J. Millis, "Collective modes and THz near field response of superconductors," *Phys. Rev. Res.*, vol. 2, p. 023413, 2020.
[14] P. B. Littlewood and C. M. Varma, "Gauge-invariant theory of the dynamical interaction of charge density waves and superconductivity" *Phys. Rev. Lett.*, vol. 47, p. 811, 1981.
[15] L. R. Walker, "Magnetostatic modes in ferromagnetic resonance," *Phys. Rev.*, vol. 105, p. 390, 1957.
[16] A. A. Allocca, Z. M. Raines, J. B. Curtis, and V. M. Galitski, "Cavity superconductor-polaritons" *Phys. Rev. B*, vol. 99, p. 020504(R), 2019.

[17] Z. Sun and A. Millis, "Bardasis–Schrieffer polaritons in excitonic insulators," *Phys. Rev. B*, vol. 102, p. 041110, 2020.
[18] H. T. Stinson, A. Sternbach, O. Najera, et al., "Imaging the nanoscale phase separation in vanadium dioxide thin films at terahertz frequencies," *Nat. Commun.*, vol. 9, p. 3604, 2018.
[19] N. G. Basov, "Semiconductor lasers," *Science*, vol. 149, p. 821, 1965.
[20] H. Deng, "Exciton-polariton Bose–Einstein condensation," *Rev. Mod. Phys.*, vol. 82, p. 1489, 2010.
[21] T. Schwartz, J. A. Hutchison, C. Genet, and T. W. Ebbesen, "Reversible switching of ultra-strong coupling," *Phys. Rev. Lett.*, vol. 106, p. 196405, 2011.
[22] S. Kéna-Cohen, S. A. Maier, and D. D. C. Bradley, "Ultrastrongly coupled exciton-polaritons in metal-clad organic semiconductor microcavities," *Adv. Opt. Mater.*, vol. 1, p. 827, 2013.
[23] L. Tian and H. J. Carmichael, "Quantum trajectory simulations of the two-state Behavior of an optical cavity containing one atom," *Phys. Rev. A*, vol. 46, p. R6801, 1992.
[24] A. Imamoğlu, H. Schmidt, G. Woods, and M. Deutsch, "Strongly interacting Photons in a nonlinear cavity," *Phys. Rev. Lett.*, vol. 79, p. 1467, 1997.
[25] J. S. Douglas, H. Habibian, C.-L. Hung, A. V. Gorshkov, H. J. Kimble and D. E. Chang, "Quantum many-body models with cold atoms coupled to photonic crystals," *Nat. Photonics*, vol. 9, p. 326, 2015.
[26] S. Dufferwiel, S. Schwarz, F. Withers, et al., "Exciton-polaritons in van der waals heterostructures embedded in tunable microcavities," *Nat. Commun.*, vol. 6, p. 8579, 2015.
[27] N. Lundt, S. Klembt, E. Cherotchenko, et al., "Room-temperature Tamm-plasmon exciton-polaritons with a WSe_2 monolayer," *Nat. Commun.*, vol. 7, p. 13328, 2016.
[28] X. Liu, T. Galfsky, Z. Sun, et al., "Strong light–matter coupling in two-dimensional atomic crystals," *Nat. Photonics*, vol. 9, p. 30, 2015.
[29] J. Sik, M. Schubert, T. Hofman and V. Gottschalch, Free-Carrier Effects and Optical Phonons in GaNAs/GaAs Superlattice Heterostructures Measured by Infrared Spectroscopic Ellipsometry, vol. 5, Cambridge University Press, 2014.
[30] E. L. Runnerstrom, K. P. Kelley, E. Sachet, C. T. Shelton, and J. P. Maria, "Epsilon-near-zero modes and surface plasmon resonance in fluorine-doped cadmium oxide thin films," *ACS Photonics*, vol. 4, p. 188, 2017.
[31] K. P. Kelley, E. L. Runnerstrom, E. Sachet, et al., "Multiple epsilon-near-zero Resonances in multilayered cadmium oxide: designing metamaterial-like optical Properties in monolithic materials," *ACS Photonics*, vol. 6, p. 1139, 2019.
[32] A. Alù, M. G. Silveirinha, A. Salandrino, and N. Engheta, "Epsilon-near-zero metamaterials and electromagnetic sources: tailoring the radiation phase pattern,"*Phys. Rev. B*, vol. 75, p. 155410, 2007.
[33] V. Bruno, C. DeVault, S. Vezzoli, et al., "Negative refraction in time-varying strongly coupled plasmonic-antenna–epsilon-near-zero systems," *Phys. Rev. Lett.*, vol. 124, p. 043902, 2020.
[34] T. G. Folland, G. Lu, A. Bruncz, J. R. Nolen, M. Tadjer, and J. D. Caldwell, "Vibrational coupling to epsilon-near-zero waveguide modes," *ACS Photonics*, vol. 7, p. 614, 2020.
[35] M. H. Javani and M. I. Stockman, "Real and imaginary Properties of epsilon-near-zero materials," *Phys. Rev. Lett.*, vol. 117, p. 107404, 2016.
[36] D. Yoo, F. de Leon-Perez, I.-H. Lee, et al., "Ultrastrong plasmon-phonon coupling via epsilon-near-zero nanocavities," arXiv: 2003.00136, 2020.
[37] A. M. Mahmoud, Y. Li, B. Edwards, and N. Engheta, "Photonic doping of epsilon-near-zero media Iñigo Liberal," *Science*, vol. 355, p. 10568, 2017.
[38] J. C. W. Song and M. S. Rudner, "Chiral plasmons without magnetic field," *Proc. Natl. Acad. Sci. U.S.A.*, vol. 113, no. 17, p. 4658, 2016.
[39] A. Kumar, A. Nemilentsau, K. Hung Fung, G. Hanson, N. X. Fang, and T. Low, "Chiral plasmon in gapped Dirac systems," *Phys. Rev. B*, vol. 93, p. 041413(R), 2016.
[40] Li-kun Shi and Justin C. W. Song, "Plasmon geometric phase and plasmon Hall shift," *Phys. Rev. X*, vol. 8, p. 021020, 2018.
[41] P. M. J. Bhaseen, M. Hohenadler, A. O. Silver, and B. D. Simons, "Polaritons and pairing Phenomena in bose-hubbard mixtures," *Phys. Rev. Lett.*, vol. 102, p. 135301, 2009.
[42] P. Cilibrizzi, H. Sigurdsson, T. C. H. Liew, et al., "Half-skyrmion spin textures in polariton microcavities," *Phys. Rev. B*, vol. 94, p. 045315, 2016.
[43] S. Donati, L. Dominici, G. Dagvadorj, et al., "Twist of generalized skyrmions and spin vortices in a polariton superfluid," *Proc. Natl. Acad. Sci. U.S.A.*, vol. 113, p. 14926, 2016.
[44] H. Hubener, U. De Giovannini, C. Schafer, et al., "Quantum cavities and Floquet materials engineering: the power of chirality," *Nat. Mater.* 2020 (in press).
[45] V. D. Vaidya, Y. Guo, R. M. Kroeze, et al., "Tunable-range, photon-mediated atomic interactions in multimode cavity QED," *Phys. Rev. X*, vol. 8, p. 011002, 2018.
[46] N. Jia, N. Schine, A. Georgakopoulos, et al., "A strongly interacting polaritonic quantum dot," *Nat. Phys.*, vol. 14, p. 550, 2018.
[47] S. Faure, C. Brimont, T. Guillet, et al., "Relaxation and emission of Bragg-mode and cavity-mode polaritons in a ZnO microcavity at room temperature," *Appl. Phys. Lett.*, vol. 95, p. 121102, 2009.
[48] D. Goldberg, L. I. Deych, A. A. Lisyansky, et al., "Exciton-lattice polaritons in multiple-quantum-well-based photonic crystals," *Nat. Photonics*, vol. 3, p. 662, 2009.
[49] E. S. Sedov, I. V. Iorsh, S. M. Arakelian, A. P. Alodjants, and A. Kavokin, "Hyperbolic metamaterials with Bragg polaritons," *Phys. Rev. Lett.*, vol. 114, p. 237402, 2015.
[50] C. Weisbuch and H. Benisty, "Microcavities in ecole polytechnique federale de lausanne, ecole polytechnique (France) and elsewhere: past, present and future," *Phys. Stat. Sol.(b)*, vol. 242, p. 2345, 2005.
[51] A. Kavokin and G. Malpuech, *Cavity Polaritons*, vol. 32, p. 246, Academic Press, 2003.
[52] P. G. Savvidis, J. J. Baumberg, R. M. Stevenson, M. S. Skolnick, D. M. Whittaker, and J. S. Roberts, "Angle-resonant stimulated polariton amplifier," *Phys. Rev. Lett.*, vol. 84, p. 1547, 2000.
[53] R. M. Stevenson, V. N. Astratov, M. S. Skolnick, et al., "Continuous wave observation of massive polariton redistribution by stimulated scattering in semiconductor microcavities," *Phys. Rev. Lett.*, vol. 85, p. 3680, 2000.
[54] H. Deng, G. Weihs, C. Santori, J. Bloch, and Y. Yamamoto, "Condensation of semiconductor microcavity exciton polaritons" *Science*, vol. 298, p. 1999, 2002.
[55] T. Guillet and C. Brimont, "Polariton condensates at room temperature," *Compt. Rendus Phys.*, vol. 17, p. 946, 2016.

[56] Á. Cuevas, J. C. López Carreño, B. Silva, et al., “First observation of the quantized exciton-polariton field and effect of interactions on a single polariton,” *Sci. Adv.*, vol. 4, p. eaao6814, 2018.
[57] A. Delteil, T. Fink, A. Schade, S. Höfling, C. Schneider, and A. İmamoğlu, “Towards polariton blockade of confined exciton-polaritons,” *Nat. Mater.*, vol. 18, p. 219, 2019.
[58] G. Muñoz-Matutano, A. Wood, M. Johnsson, et al., “Emergence of quantum correlations from interacting fibre-cavity polaritons,” *Nat. Mater.*, vol. 18, p. 213, 2019.
[59] S. S. Demirchyan, Y. Chestnov, A. P. Alodjants, M. M. Glazov, and A. V. Kavokin, “Qubits Based on polariton Rabi oscillators,” *Phys. Rev. Lett.*, vol. 112, p. 196403, 2014.
[60] I. V. Novikov and A. A. Maradudin, “Channel polaritons” *Phys. Rev. B*, vol. 66, p. 035403, 2002.
[61] S. I. Bozhevolnyi, V. S. Volkov, E. Devaux, J-Y. Laluet, and T. W. Ebbesen, “Channel plasmon subwavelength waveguide components including interferometers and ring resonators,” *Nature*, vol. 440, p. 508, 2006.
[62] P. A. D. Gonçalves, S. Xiao, N. M. R. Peres, and N. Asger Mortensen, “Hybridized plasmons in 2D nanoslits: from Graphene to anisotropic 2D materials,” *ACS Photonics*, vol. 4, p. 3045, 2017.
[63] Z. Fei, A. S. Rodin, G. O. Andreev, et al., “Gate-tuning of graphene plasmons revealed by infrared nano-imaging,” *Nature*, vol. 487, p. 82, 2012.
[64] J. Chen, M. Badioli, P. Alonso-Gonzalez, et al., “Optical nano-imaging of gate-tunable graphene plasmons,” *Nature*, vol. 487, p. 77, 2012.
[65] M. D. Goldflam, G.-X. Ni, K. W. Post, et al., “Tuning and persistent switching of graphene plasmons on a ferroelectric substrate,” *Nano Lett.*, vol. 15, p. 4859, 2015.
[66] S. Xiao, X. Zhu, B.-H. Li, and N. Asger Mortensen, “Graphene-plasmon polaritons: from fundamental properties to potential applications,” *Front. Phys.*, vol. 11, p. 117801, 2016.
[67] M. Wagner, Z. Fei, A. S. McLeod, et al., “Ultrafast and nanoscale plasmonic phenomena in exfoliated graphene revealed by infrared pump–probe nanoscopy,” *Nano Lett.*, vol. 14, p. 894, 2014.
[68] D. J. Rizzo, B. S. Jessen, Z. Sun, et al., “Graphene/α-RuCl3: an emergent 2D plasmonic interface,” arXiv:2007.07147, 2020.
[69] F. Wen, Y. Zhang, S. Gottheim, et al., “Charge transfer plasmons: optical frequency Conductances and tunable infrared resonances,” *ACS Nano*, vol. 9, p. 6428, 2015.
[70] M. Forg, L. Colombier, R. K. Patel, et al., “Cavity-control of interlayer excitons in van der Waals heterostructures,” *Nat. Commun.*, vol. 10, p. 3697, 2019.
[71] R. Rapaport, R. Harel, E. Cohen, A. Ron, E. Linder, and L. N. Pfeiffer, “Negatively charged quantum well Polaritons in a GaAs/AlAs microcavity: an analog of atoms in a cavity,” *Phys. Rev. Lett.*, vol. 84, p. 1607, 2000.
[72] J. M. Raimond and S. Haroche, “Confined electrons and photons,” edited by E. Burstein and C. Weisbuch, *Springer- New Physics and Applications*, vol. 383, 1995.
[73] A. Tiene, J. Levinsen, M. M. Parish, A. H. MacDonald, J. Keeling, and F. M. Marchetti, “Extremely imbalanced two-dimensional electron–hole–photon systems,” *Phys. Rev. Res.*, vol. 2, p. 023089, 2020.
[74] P. A. Cherenkov. "Visible emission of clean liquids by action of γ radiation,” *Dokl. Akad. Nauk SSSR*, vol. 2, p. 451, 1934.
[75] P. Genevet, D. Wintz, A. Ambrosio, A. She, R. Blanchard and F. Capasso, “Controlled steering of Cherenkov surface plasmon wakes with a one-dimensional metamaterial,” *Nat. Nanotechnol.*, vol. 10, p. 804, 2015.
[76] D. H. Auston, K. P. Cheung, J. A. Valdmanis, and D. A. Kleinman, “Cherenkov radiation from femtosecond optical pulses in electro-optic media,” *Phys. Rev. Lett.*, vol. 53, p. 1555, 1984.
[77] C. Maciel-Escudero, A. Konĕcńa, R. Hillenbrand, and J. Aizpurua, “Probing and steering bulk and surface phonon polaritons in uniaxial materials using fast electrons: hexagonal boron nitride,” arXiv:2006.05359v1, 2020.
[78] Y. Zhang, C. Hu, B. Lyu, et al., “Tunable Cherenkov radiation of phonon Polaritons in silver nanowire/hexagonal boron nitride heterostructures,” *Nano Lett.*, vol. 20, p. 2770, 2020.
[79] H. T. Stinson, J. S. Wu, B. Y. Jiang, et al., “Infrared nanospectroscopy and imaging of collective superfluid excitations in anisotropic superconductors,” *Phys. Rev. B*, vol. 90, p. 014502, 2014.
[80] A. Dodel, A. Pikovski, I. Ermakov, et al., “Cooper pair polaritons in cold fermionic atoms within a cavity,” *Phys. Rev. Res.*, vol. 2, p. 013184, 2020.
[81] W. L. Barnes, A. Dereux, D T. W. Ebbesen, “Surface plasmon subwavelength optics,” *Nature*, vol. 424, p. 824, 2003.
[82] P. J. Schuck, D. P. Fromm, A. Sundaramurthy, G. S. Kino, and W. E. Moerner, “Improving the mismatch between light and nanoscale objects with gold bowtie nanoantennas,” *Phys. Rev. Lett.*, vol. 94, p. 017402, 2005.
[83] P. Biagioni, J. S. Huang, and B. Hecht, “Nanoantennas for visible and infrared radiation,” *Rep. Prog. Phys.*, vol. 75, p. 024402, 2012.
[84] L. Novotny and N. Van Hulst, “Antennas for light,” *Nat. Photonics*, vol. 5, p. 83, 2011.
[85] J. J. Baumberg, J. Aizpurua, M. H. Mikkelsen, and D. R. Smith, “Extreme nanophotonics from ultrathin metallic gaps,” *Nat. Mater.*, vol. 18, p. 668, 2019.
[86] M. Tamagnone, A. Ambrosio, K. Chaudhary, et al., “Ultra-confined mid-infrared resonant phonon polaritons in van der Waals nanostructures,” *Sci. Adv.*, vol. 4, p. eaat7189, 2018.
[87] A. M. Dubrovkin, B. Qiang, T. Salim, D. Nam, N. I. Zheludey and Q. J. Wang, “Resonant nanostructures for highly confined and ultra-sensitive surface phonon-laritons,” *Nat. Commun.*, vol. 11, p. 1863, 2020.
[88] L. V. Brown, M. Davanco, Z. Sun, et al., “Nanoscale mapping and spectroscopy of nonradiative hyperbolic modes in hexagonal boron nitride nanostructures,” *Nano Lett.*, vol. 18, p. 1628, 2018.
[89] X. Chen, D. Hu, R. Mescall, et al., “Modern scattering-type scanning near-field optical microscope for advanced material research,” *Adv. Mater.*, vol. 31, p. 1804774, 2019.
[90] Z. Fei, G. O. Andreev, W. Bao, et al., “Infrared nanoscopy of Dirac plasmons at the graphene–SiO_2 interface,” *Nano Lett.*, vol. 11, p. 4701, 2011.
[91] P. J. Schuck, A. Weber-Bargioni, P. D. Ashby, D. F. Ogletree, A. Schwartzberg, and S. Cabrini, “Life beyond diffraction: opening new routes to materials characterization with next-generation optical near-field approaches,” *Adv. Funct. Mater.*, vol. 23, p. 2539, 2013.
[92] S. Berweger, J. M. Atkin, R. L. Olmon, and M. B. Raschke, “Light on the tip of a needle: plasmonic nanofocusing for spectroscopy on the nanoscale,” *J. Phys. Chem. Lett.*, vol. 3, p. 945, 2012.

[93] K. D. Park, T. Jiang, G. Clark, X. Xu, M. B. Raschke, "Radiative control of dark excitons at room temperature by nano-optical antenna-tip Purcell effect," *Nat. Nanotechnol.*, vol. 13, p. 59, 2017.
[94] B.-Y. Jiang, L. M. Zhang, A. H. Castro Neto, D. N. Basov, and M. M. Fogler, "Generalized spectral method for near-field optical microscopy," *J. Appl. Phys.*, vol. 119, p. 054305, 2016.
[95] F. Keilmann and R. Hillenbrand, "Near-field microscopy by elastic light scattering from a tip," *J. Philos. Trans. R. Soc. Lond. Ser. A Math. Phys. Eng. Sci.*, vol. 362, p. 787, 2014.
[96] J. M. Atkin, S. Berweger, A. C. Jones and M. B. Raschke, "Nano-optical imaging and spectroscopy of order, phases, and domains in complex solids," *Adv. Phys.*, vol. 61, p. 745, 2012.
[97] M. Fleischhauer and M. D. Lukin, "Dark-state polaritons in electromagnetically induced transparency," *Phys. Rev. Lett.*, vol. 84, p. 5094, 2000.
[98] S. E. Harris, J. E. Field, and A. Imamoglu, "Nonlinear optical processes using electromagnetically induced transparency," *Phys. Rev. Lett.*, vol. 64, p. 1107, 1990.
[99] M. D. Lukin, "Colloquium: trapping and manipulating photon states in atomic ensembles," *Rev. Mod. Phys.*, vol. 75, p. 457, 2003.
[100] M. Fleischhauer, A. Imamoglu and J. P. Marangos, "Electromagnetically induced transparency: optics in coherent media," *Rev. Mod. Phys.*, vol. 77, p. 633, 2005.
[101] H. Zoubi and H. Ritsch, "Lifetime and emission characteristics of collective electronic excitations in two-dimensional optical lattices," *Phys. Rev. A*, vol. 83, p. 063831, 2011.
[102] R. J. Bettles, S. A. Gardiner, and C. S. Adams, "Cooperative eigenmodes and scattering in one-dimensional atomic arrays," *Phys. Rev. A*, vol. 94, p. 043844, 2016.
[103] A. Asenjo-Garcia, M. Moreno-Cardoner, A. Albrecht, H. J. Kimble, and D. E. Chang, "Exponential improvement in photon storage fidelities using subradiance and "selective radiance," in atomic arrays" *Phys. Rev. X*, vol. 7, p. 031024, 2017.
[104] E. Shahmoon, D. S. Wild, M. D. Lukin, and S. F. Yelin, "Cooperative resonances in light scattering from two-dimensional atomic arrays," *Phys. Rev. Lett.*, vol. 118, p. 113601, 2017.
[105] D. Pines, "Electron Interaction in solids," *Can. J. Phys.*, vol. 34, p. 1379, 1956.
[106] Z. Sun, D. N. Basov, and M. M. Fogler, "Universal linear and nonlinear electrodynamics of a Dirac fluid," *Proc. Natl. Acad. Sci. U.S.A.*, vol. 115, p. 3285, 2018.
[107] Z. Sun, D. N. Basov, and M. M. Fogler, "Adiabatic amplification of plasmons and demons in 2D systems," *Phys. Rev. Lett.*, vol. 117, p. 076805, 2016.
[108] M. Jablan, H. Buljan, and M. Soljačić, "Plasmonics in graphene at infrared frequencies," *Phys. Rev. B*, vol. 80, p. 245435, 2009.
[109] A. Woessner, M. B. Lundeberg, Y. Gao, et al., "Highly confined low-loss plasmons in graphene-boron nitride heterostructures," *Nat. Mater.*, vol. 14, p. 421, 2015.
[110] G. X. Ni, A. S. McLeod, Z. Sun, et al., "Fundamental limits to graphene plasmonics," *Nature*, vol. 557, p. 530, 2018.
[111] M. I. Dyakonov, "New type of electromagnetic wave propagating at an interface," *Sov. Phys. JETP*, vol. 67, p. 714, 1988.
[112] O. Takayama, L. Crasovan, D. Artigas, and L. Torner, "Observation of Dyakonov surface waves," *Phys. Rev. Lett.*, vol. 102, p. 043903, 2009.
[113] J. Zubin and E. E. Narimanov, "Optical hyperspace for plasmons: Dyakonov states in metamaterials," *Appl. Phys. Lett.*, vol. 93, p. 221109, 2008.
[114] S. Dai, M. Tymchenko, Y. Yang, et al., "Manipulation and steering of hyperbolic surface polaritons in hexagonal boron nitride," *Adv. Mater.*, vol. 30, p. 1706358, 2018.
[115] F. J. Alfaro-Mozaz, P. Alonso-Gonzalez, S. Velez, et al., "Nanoimaging of resonating hyperbolic polaritons in linear boron nitride antennas," *Nat. Commun.*, vol. 8, p. 15624, 2017.
[116] I. Dolado, F. J. Alfaro-Mozaz, P. Li, et al., "Nanoscale guiding of infrared light with hyperbolic volume and surface polaritons in van der Waals material ribbons," *Adv. Mater.*, vol. 32, p. 1906530, 2020.
[117] D. B. Mast, A. J. Dahm, and A. L. Fetter, "Observation of bulk and edge magnetoylasmons in a two-dimensional electron fluid," *Phys. Rev. Lett.*, vol. 54, p. 1706, 1985.
[118] V. A. Volkov and S. A. Mikhailov, "Edge magnetoplasmons: low frequency weakly damped excitations in inhomogeneous two-dimensional electron systems," *Radio Eng. Electron. Inst. USSR Acad. Sci. Zh. Eksp. Teor. Fiz.*, vol. 94, p. 217, 1988.
[119] N. Kumada, P. Roulleau, B. Roche, et al., "Resonant edge magnetoplasmons and their decay in graphene," *Phys. Rev. Lett.*, vol. 113, p. 266601, 2014.
[120] I. Petkovic, F. I. B. Williams and D. Christian Glattli, "Edge magnetoplasmons in graphene," *J. Phys. D Appl. Phys.*, vol. 47, 2014.
[121] M. L. Sadowski, G. Martinez, M. Potemski, C. Berger, and W. A. de Heer, "Landau level spectroscopy of ultrathin graphite layers," *Phys. Rev. Lett.*, vol. 97, p. 266405, 2006.
[122] Z. Jiang, E. A. Henriksen, L. C. Tung, et al., "Infrared spectroscopy of Landau levels in graphene," *Phys. Rev. Lett.*, vol. 98, p. 197403, 2007.
[123] M. Orlita, C. Faugeras, R. Grill, et al., "Carrier scattering from dynamical magneto-conductivity in quasineutral epitaxial graphene," *Phys. Rev. Lett.*, vol. 107, p. 216603, 2011.
[124] Z. G. Chen, Z. Shi, W. Yang, et al., "Observation of an intrinsic bandgap and Landau level renormalization in graphene/boron-nitride heterostructures," *Nat. Commun.*, vol. 5, p. 4461, 2014.
[125] I. O. Nedoliuk, S. Hu, A. K. Geim, and A. B. Kuzmenko, "Colossal infrared and terahertz magneto-optical activity in a two-dimensional Dirac material,"*Nat. Nano*, vol. 14, p. 756, 2019.
[126] Z. Fei, M. D. Goldflam, J.-S. Wu, et al., "Edge and surface plasmons in graphene nanoribbons," *Nano Lett.*, vol. 15, pp. 8271–8276, 2015.
[127] P. Li, I. Dolado, F. J. Alfaro-Mozaz, et al., "Optical nanoimaging of hyperbolic surface polaritons at the Edges of van der Waals materials," *Nano Lett.*, vol. 17, p. 228, 2017.
[128] A. Y. Nikitin, P. Alonso-González, S. Vélez, et al., "Real-space mapping of tailored sheet and edge plasmons in graphene nanoresonators," *Nat. Photonics*, vol. 10, p. 239, 2016.
[129] P. Berini, "Plasmon-polariton waves guided by thin lossy metal films of finite width: Bound modes of symmetric structures," *Phys. Rev. B*, vol. 61, p. 10484, 2000.
[130] M. Lorente-Crespo, G. C. Ballesteros, C. Mateo-Segura, and C. García-Meca, "Edge-plasmon whispering-gallery modes in nanoholes" *Phys. Rev. Appl.*, vol. 13, p. 024050, 2020.
[131] T. Rindzevicius, Y. Alaverdyan, B. Sepulveda, et al., "Nanohole plasmons in optically thin gold films," *J. Phys. Chem. C*, vol. 111, p. 1207, 2007.

[132] A. Degiron, H. Lezec, N. Yamamoto, and T. Ebbe-sen, "Optical transmission properties of a single subwave-length aperture in a real metal," *Opt. Commun*, vol. 239, p. 61, 2004.
[133] N. Liu, L. Langguth, T. Weiss, et al., "Plasmonic analogue of electromagnetically induced transparency at the Drude damping limit," *Nat. Mater.*, vol. 8, p. 758, 2009.
[134] R. Taubert, M. Hentschel, J. Kastel, and H. Gissen, "Classical analog of electromagnetically induced absorption in plasmonics," *Nano Lett.*, vol. 12, p. 1367, 2012.
[135] H. Yan, T. Low, F. Guinea, F. Xia, and P. Avouris, "Tunable phonon-induced transparency in bilayer graphene nanoribbons," *Nano Lett.*, vol. 14, p. 4581, 2014.
[136] S. Xia, X. Zhai, L. Wang, and S. Wen, "Plasmonically induced transparency in in-plane isotropic and anisotropic 2D materials," *Opt. Express*, vol. 28, p. 7980, 2020.
[137] V. Walther, R. Johne and T. Pohl, "Giant optical nonlinearities from Rydberg excitons in semiconductor microcavities," *Nat. Commun.*, vol. 9, p. 1309, 2018.
[138] C. Weisbuch, M. Nishioka, A. Ishikawa, and Y. Arakawa, "Observation of the coupled exciton-photon mode splitting in a semiconductor quantum microcavity," *Phys. Rev. Lett.*, vol. 69, p. 3314, 1992.
[139] J. Kasprzak, M. Richard, S. Kundermann, et al., "Bose–Einstein condensation of exciton polaritons" *Nature*, vol. 443, p. 409, 2006.
[140] I. Carusotto and C. Ciuti, "Quantum fluids of light," *Rev. Mod. Phys*, vol. 85, p. 29,2013.
[141] T. Byrnes, N. Y. Kim, and Y. Yamamoto, "Exciton-polariton condensates," *Nat. Phys.*, vol. 10, p. 803, 2014.
[142] A. Griffin, D. W. Snoke, and S. Stringari, eds., *Bose–Einstein Condensation*, Cambridge University Press, 1996.
[143] A. A. High, J. R. Leonard, A. T. Hammack, et al., "Spontaneous coherence in a cold exciton gas," *Nature*, vol. 483, p. 7391, 2012.
[144] D. Snoke, "Spontaneous Bose coherence of excitons and polaritons," *Science*, vol. 298, p. 1368, 2002.
[145] J. P. Eisenstein and A. H. MacDonald, "Bose–Einstein condensation of excitons in bilayer electron systems," *Nature*, vol. 432, p. 691, 2004.
[146] H. Deng, H. Haug, and Y. Yamamoto, "Exciton-polariton Bose-Einstein condensation," *Rev. Mod. Phys.*, vol. 82, p. 1489, 2010.
[147] D. W. Snoke and J. Keeling, "The new era of polariton condensates," *Phys. Today*, vol. 70, p. 54, 2017.
[148] Y. Sun, P. Wen, Y. Yoon, et al., "Bose–Einstein condensation of long-lifetime polaritons in thermal equilibrium," *Phys. Rev. Lett.*, vol. 118, p. 016602, 2017.
[149] G. Lerario, A. Fieramosca, F. Barachati, et al., "Room-temperature superfluidity in a polariton condensate," *Nat. Phys.*, vol. 13, p. 837, 2013.
[150] Y. Fu, H. Zhu, J. Chen, M. P. Hautzinger, X.-Y. Zhu, and S. Jin, "Metal halide perovskite nanostructures for optoelectronic applications and the study of physical properties," *Nat. Rev. Mater.*, vol. 4, p. 169, 2019.
[151] A. T. Hanbicki, M. Currie, G. Kioseoglou, A. L. Friedman, and B. T. Jonker, "Measurement of high exciton binding energy in the monolayer transition-metal dichalcogenides WS_2 and WSe_2," *Sol. State. Commun.*, vol. 203, p. 16, 2015.
[152] T. Cheiwchanchamnangij and W. R. L. Lambrecht, "Quasiparticle band structure calculation of monolayer, bilayer, and bulk MoS_2," *Phys. Rev. B*, vol. 85, p. 205302, 2012.
[153] A. Ramasubramaniam, "Large excitonic effects in monolayers of molybdenum and tungsten dichalcogenides," *Phys. Rev. B*, vol. 86, p. 115409, 2012.
[154] H.-P. Komsa and A. V. Krasheninnikov, "Effects of confinement and environment on the electronic structure and exciton binding energy of MoS_2 from first principles," *Phys. Rev. B*, vol. 86, p. 241201, 2012.
[155] Y. Liang, S. Huang, R. Soklaski, and L. Yang, "Quasiparticle band-edge energy and band offsets of monolayer of molybdenum and tungsten chalcogenides," *Appl. Phys. Lett.*, vol. 103, p. 042106, 2013.
[156] K. He, N. Kumar, L. Zhao, et al., "Tightly bound excitons in monolayer WSe_2," *Phys. Rev. Lett.*, vol. 113, p. 026803, 2014.
[157] Z. Ye, T. Cao, K. O'Brien, et al., "Probing excitonic dark states in single-layer tungsten disulphide," *Nature*, vol. 513, p. 214, 2014.
[158] K. Yao, A. Yan, S. Kahn, et al., "Optically discriminating carrier-induced quasiparticle band gap and exciton energy renormalization in monolayer MoS_2," *Phys. Rev. Lett.*, vol. 119, p. 087401, 2017.
[159] H. Min, R. Bistritzer, J. Su and A. H. MacDonald, "Room-temperature superfluidity in graphene bilayers" *Phys. Rev. B*, vol. 78, p. 121401, 2008.
[160] M. M. Fogler, L. V. Butov, and K. S. Novoselov, "High-temperature superfluidity with indirect excitons in van der Waals heterostructures" *Nat. Commun.*, vol. 5, p. 4555, 2014.
[161] F.-C. Wu, F. Xue, and A. H. MacDonald, "Theory of two-dimensional spatially indirect equilibrium exciton condensates," *Phys. Rev. B*, vol. 92, p. 165121, 2015.
[162] A. V. Nalitov, H. Sigurdsson, S. Morina, et al., "Optically trapped polariton condensates as semiclassical time crystals," *Phys. Rev. A*, vol. 99, p. 033830, 2019.
[163] M. D. Fraser, S. Hofling, and Y. Yamamoto, "Physics and applications of exciton-polariton lasers," *Nat. Mater.*, vol. 15, p. 1049, 2016.
[164] A. Gianfrate, L. Dominici, O. Voronych, et al., "Superluminal X-waves in a polariton quantum fluid," *Light Sci. Appl.*, vol. 7, p. 17119, 2018.
[165] A. Gabbay, Y. Preezant, E. Cohen, B. M. Ashkinadze and L. N. Pfeffier, "Fermi edge Polaritons in a microcavity containing a high-density two-dimensional electron gas,"*Phys. Rev. Lett.*, vol. 99, p. 157402, 2007.
[166] D. Pimenov, J. von Delft, L. Glazman, and M. Goldstein, "Fermi-edge exciton-polaritons in doped semiconductor microcavities with finite hole mass," *Phys. Rev. B*, vol. 96, p. 155310, 2017.
[167] M. Baetena and M. Wouters, "Mahan polaritons and their lifetime due to hole recoil," *Eur. Phys. J. D*, vol. 69, p. 243, 2015.
[168] G. D. Mahan, "Excitons in degenerate semiconductors," *Phys. Rev.*, vol. 153, p. 882, 1967.
[169] G. D. Mahan, "Excitons in metals" *Phys. Rev. Lett.*, vol. 18, p. 448, 1967.
[170] T. Oka and S. Kitamura, "Floquet engineering of quantum materials," *Ann. Rev. Condensed Matter Phys.*, vol. 10, p. 387, 2019.
[171] L. W. Clark, N. Jia, N. Schine, C. Baum, A. Georgakopoulos, and J. Simon, "Interacting Floquet polaritons," *Nature*, vol. 571, p. 532, 2019.
[172] F. Mahmood, C.-K. Chan, Z. Alpichshev, et al., "Selective scattering between Floquet-Bloch and Volkov states in a topological insulator," *Nat. Phys.*, vol. 12, p. 306, 2016.

[173] H. Hübener, U. D. Giovannini, and A. Rubio, "Phonon driven Floquet matter," *Nano Lett.*, vol. 18, p. 1535, 2018.
[174] J.-M. Ménard, C. Poellmann, M. Porer, et al., "Revealing the dark side of a bright exciton-polariton condensate," *Nat. Commun.*, vol. 5, p. 4648, 2018.
[175] Z. Sun, J. Gu, A. Ghazaryan, et al., "Optical control of room-temperature valley polaritons," *Nat. Photonics*, vol. 11, p. 491, 2017.
[176] L. Vestergaard Hau, S. E. Harris, Z. Dutton, and C. H. Behroozi, "Light speed reduction to 17 metres per second in an ultracold atomic gas," *Nature*, vol. 397, p. 594, 1999.
[177] O. Kocharovskaya, Y. Rostovtsev, and M. O. Scully, "Stopping light via hot atoms," *Phys. Rev. Lett.*, vol. 86, p. 628, 2001.
[178] M. Bajcsy, A. S. Zibrov, and M. D. Lukin, "Stationary pulses of light in an atomic medium," *Nature*, vol. 426, p. 638, 2003.
[179] S. Betzold, M. Dusel, O. Kyriienko, et al., "Coherence and Interaction in confined room-temperature polariton condensates with Frenkel excitons," *ACS Photonics*, vol. 7, p. 384, 2020.
[180] D. G. Lidzey, D. D. C. Bradley, T. Virgili, S. Walker, and D. M. Walker, "Strong exciton–photon coupling in an organic semiconductor microcavity," *Nature*, vol. 395, p. 53, 1998.
[181] G. Lerario, A. Fieramosca, F. Barachati, et al., "Room-temperature superfluidity in a polariton condensate," *Nat. Phys.*, vol. 13, p. 837, 2017.
[182] J. Keeling and S. Kena-Cohen, "Bose–Einstein condensation of exciton-polariton in organic microcavities," *Annu. Rev. Phys. Chem.*, vol. 71, p. 435, 2020.
[183] S. Foteinopoulou, G. Chinna Rao Devarapu, G. S. Subramania, S. Krishna and D. Wasserman, "Phonon-polaritonics: enabling powerful capabilities for infrared photonics," *Nanophotonics*, vol. 8, p. 2129, 2019.
[184] K. I. Kliewer and R. Fuchs, "Optical modes of vibration in an ionic crystal slab including retardation. I. Nonradiative region," *Phys. Rev.*, vol. 144, p. 495, 1966.
[185] A. Huber, N. Ocelic, D. V. Kazantsev, and R. Hillenbrand, "Near-field imaging of mid-infrared surface phonon polariton propagation," *Appl. Phys. Lett.*, vol. 87, p. 081103, 2005.
[186] R. Hillenbrand, T. Taubner and F. Keilmann, "Phonon-enhanced light-matter interaction at the nanometre scale," *Nature*, vol. 418, p. 159, 2002.
[187] J. D. Caldwell, O. J. Glembocki, N. Sharac, et al., "Low-loss, extreme sub-diffraction photon confinement via silicon carbide surface phonon polariton nanopillar resonators," *Nano Lett.*, vol. 13, p. 3690, 2013.
[188] T. E. Tiwald, J. A. Woolam, S. Zollner, et al., "Carrier concentration and lattice absorption in bulk and epitaxial silicon carbide determined using infrared ellipsometry," *Phys. Rev. B*, vol. 60, p. 11464, 1999.
[189] T. Taubner, D. Korobkin, Y. Urzhumov, G. Shvets, and R. Hillenbrand, "Near-field microscopy through a SiC superlens," *Science*, vol. 313, p. 1595, 2006.
[190] W. J. Moore and R. T. Holm. "Infrared dielectric constant of GaAs," *J. Appl. Phys.*, vol. 80, p. 6939, 1996.
[191] M. Francesco, D. Pellegrino, M. I. Katsnelson, and M. Polini, "Helicons in Weyl semimetals," *Phys. Rev. B*, vol. 92, p. 201407, 2015.
[192] J. Zhou, H.-R. Chang, and D. Xiao, "Plasmon mode as a detection of the chiral anomaly in Weyl semimetals," *Phys. Rev. B*, vol. 91, p. 035114, 2015.
[193] C. Justin W. Song, and M. S. Rudner, "Fermi arc plasmons in Weyl semimetals," *Phys. Rev. B*, vol. 96, p. 205443, 2017.
[194] I. Iorsh, G. Rahmanova, and M. Titov, "Plasmon-polariton from a helical state in a Dirac magnet," *ACS Photonics*, vol. 6, p. 2450, 2019.
[195] J. Lin, J. P. Bathasar Mueller, Q. Wang, et al., "Polarization-controlled tunable directional coupling of surface plasmon polaritons," *Science*, vol. 340, p. 331, 2013.
[196] L. Huang, X. Chen, B. Bai, et al., "Helicity dependent directional surface plasmon polariton excitation using a metasurface with interfacial phase discontinuity," *Light Sci. Appl.*, vol. 2, p. 70, 2013.
[197] J. J. Hopfield, "Theory of the contribution of excitons to the complex dielectric constant of crystals," *Phys. Rev.*, vol. 112, p. 1555, 1958.
[198] C. H. Henry and J. J. Hopfield, "Raman scattering by polaritons," *Phys. Rev. Lett.*, vol. 15, p. 964, 1965.
[199] U. Fano, "Atomic theory of electromagnetic interactions in dense materials," *Phys. Rev.*, vol. 103, p. 1202, 1956.
[200] K. Huang, "Lattice vibrations and optical waves in ionic crystals," *Nature*, vol. 167, p. 779, 1951.
[201] K. B. Tolpygo, "Physical properties of a rock salt lattice made up of deformeable ions," Translated and reprinted from *Zh. Eksp. Teor. Fiz.*, vol. 20, no. 6, p. 497, 1950.
[202] J. D. Caldwell, I. Vurgaftman, J. G. Tischler, O. J. Glembocki, J. C. Owrutsky, and T. L. Reinecke, "Atomic-scale photonic hybrids for mid-infrared and terahertz nanophotonics," *Nat. Nanotechnol.*, vol. 11, p. 9, 2016.
[203] L. Wendler and R. Haupt, "Long-range surface plasmon-phonon-polaritons," *J. Phys. C Solid State Phys.*, vol. 19, p. 1871, 1986.
[204] B. Askenazi, A. Vasanelli, A. Delteil, et al., "Ultra-strong light–matter coupling for designer Reststrahlen band," *New J. Phys.*, vol. 16, p. 043029, 2014.
[205] C. Franckié, K. Ndebeka-Bandou, J. Ohtani, and M. Faist, "Quantum model of gain in phonon-polariton lasers," *Phys. Rev. B*, vol. 97, p. 075402, 2018.
[206] N. C. Passler, C. R. Gubbin, T. G. Folland, et al., "Strong coupling of epsilon-near-zero phonon Polaritons in polar dielectric heterostructures," *Nano Lett.*, vol. 18, p. 428, 2018.
[207] A. A. Strashko and V. M. Agranovich, "To the theory of surface plasmon-polaritons on metals covered with resonant thin films," *Opt. Commun.*, vol. 332, p. 201, 2014.
[208] D. C. Ratchford, C. J. Winta, I. Chatzakis, et al., "Controlling the infrared dielectric function through atomic-scale heterostructures," *ACS Nano*, vol. 13, p. 6730, 2019.
[209] E. L. Runnerstrom, K. P. Kelley, T. G. Folland, et al., "Polaritonic hybrid-epsilon-near-zero modes: beating the plasmonic confinement vs propagation-length trade-off with doped cadmium oxide bilayers," Nano Lett., vol. 19, p. 948, 2019.
[210] K. Chaudhary, M. Tamagnone, M. Resaee, et al., "Engineering phonon polaritons in van der Waals heterostructures to enhance in-plane optical anisotropy," *Sci. Adv.*, vol. 5, p. eaau7171, 2019.

[211] S. Dai, Q. Ma, M. K. Liu, et al., “Graphene on hexagonal boron nitride as a tunable hyperbolic metamaterial,” *Nat. Nanotechnol.*, vol. 10, p. 682, 2015.

[212] F. J. Bezares, A. De Sanctis, J. R. M. Saavedra, et al., “Intrinsic plasmon-phonon interactions in highly doped graphene: a near-field imaging study,” *Nano Lett.*, vol. 17, p. 5908, 2017.

[213] A. Kumar, T. Low, K. Hung Fung, P. Avouris, and N. X. Fang, “Tunable light–matter interaction and the role of hyperbolicity in graphene-hBN system,” *Nano Lett.*, vol. 15, p. 3172, 2015.

[214] A. T. Costa, P. A. D. Gonçalves, H. Frank, et al., “Harnessing ultra-confined graphene plasmons to probe the electrodynamics of superconductors,” arXiv:2006.00748, 2020.

[215] H. Dehghani, Z. M. Raines, V. M. Galitski, and M. Hafezi, “Optical enhancement of superconductivity via targeted destruction of charge density waves,” *Phys. Rev. B*, vol. 101. p. 195106, 2020.

[216] D. Rodrigo, O. Limaj, D. Janner, et al., “Mid-infrared plasmonic biosensing with graphene,” *Science*, vol. 349, p. 165, 2015.

[217] M. Autore, P. Li, I. Dolado, et al., “Boron nitride nanoresonators for phonon-enhanced molecular vibrational spectroscopy at the strong coupling limit,” *Light Sci. Appl.*, vol. 7, p. 17172, 2018.

[218] C. R. Gubbin, R. Berte, M. A. Meeker, et al., “Hybrid longitudinal-transverse phonon polaritons,” *Nat. Commun.*, vol. 10, p. 1682, 2019.

[219] T. G. Folland, A. Fali, S. T. White, et al., “Reconfigurable infrared hyperbolic metasurfaces using phase change materials,” *Nat. Commun.*, vol. 9, p. 4371, 2018.

[220] A. Poddubny, I. Iorsh, P. Belov, and Y. Kivshar, “Hyperbolic metamaterials,” *Nat. Photonics*, vol. 7, p. 948, 2013.

[221] J. S. Gomez-Diaz and A. Alu, “Flatland optics with hyperbolic metasurfaces,” *ACS Photonics*, vol. 3, p. 2211, 2016.

[222] J. S. Gomez-Diaz, M. Tymchenko, and A. Alù, “Hyperbolic plasmons and topological transitions over uniaxial metasurfaces,” *Phys. Rev. Lett.*, vol. 114, p. 233901, 2015.

[223] J. D. Caldwell, A. V. Kretinin, Y. Chen, et al., “Sub-diffractional volume-confined polaritons in the natural hyperbolic material hexagonal boron nitride,” *Nat. Commun.*, vol. 5, p. 5221, 2014.

[224] Y. Guo, W. Newman, C. L. Cortes, and Z. Jacob, “Applications of hyperbolic metamaterial substrates,” *Adv. Optoelectron.* 452502, (2012).

[225] C. L. Cortes, W. Newman, S. Molesky and Z. Jacob “Quantum nanophotonics using hyperbolic metamaterials,” *J. Opt.*, vol. 14, p. 063001, 2012.

[226] J. Sun, N. M. Litchinitser, and J. Zhou, “Indefinite by nature: from ultraviolet to terahertz,” *ACS Photonics*, vol. 1, p. 293, 2014.

[227] E. E. Narimanov and A. V. Kildishev, “Metamaterials naturally hyperbolic,” *Nat. Photonics*, vol. 9, p. 214, 2015.

[228] S. Dai, Z. Fei, Q. Ma, et al., “Tunable phonon polaritons in atomically thin van der Waals crystals of boron nitride,” *Science*, vol. 343, p. 1125, 2014.

[229] A. J. Giles, S. Dai, I. Vurgaftman, et al., “Ultralow-loss polaritons in isotopically pure boron nitride,” *Nat. Mater.*, vol. 17, p. 134, 2017.

[230] J. Taboada-Gutiérrez, G. Álvarez-Pérez, J. Duan, et al., “Broad spectral tuning of ultra-low-loss polaritons in a van der Waals crystal by intercalation,” *Nat. Mater.*, vol. 19, p. 964, 2020.

[231] J. D. Caldwell, I. Aharonovich, G. Cassabois, J. H. Edgar, B. Gil and D. N. Basov, “Photonics with hexagonal boron nitride” *Nat. Mater. Rev.*, vol. 4, no. 8, p. 552, 2019.

[232] A. Fali, S. T. White, T. G. Folland, et al., “Refractive index-based Control of hyperbolic phonon-polariton propagation,” *Nano Lett.*, vol. 9, no. 11, 7725–7730, 2019.

[233] A. Ambrosio, L. A. Jauregui, S. Dai, et al., “Mechanical detection and imaging of hyperbolic phonon polaritons in hexagonal boron nitride,” *ACS Nano*, vol. 11, p. 8741, 2017.

[234] A. Ambrosio, M. Tamagnone, K. Chaudhary, et al., “Selective excitation and imaging of ultraslow phonon polaritons in thin hexagonal boron nitride crystals,” *Light Sci. Appl.*, vol. 7, p. 27, 2018.

[235] G. Hu, J. Shen, C. W. Qiu, A. Alù, and S. Dai, “Phonon Polaritons and hyperbolic Response in van der waals materials,” *Adv. Opt. Mater. Spec. Issue Polarit. Nanomater.*, vol. 8, p. 1901393, 2020.

[236] S. Dai, J. Quan, G. Hu, et al., “Hyperbolic phonon polaritons in suspended hexagonal boron nitride,” *Nano Lett.*, vol. 19, p. 100, 2019.

[237] S. Dai, M. Tymchenko, Z. Q. Xu, et al., “Internal nanostructure diagnosis with hyperbolic phonon polaritons in hexagonal boron nitride,” *Nano Lett.*, vol. 18, p. 5205, 2018.

[238] A. J. Hoffman, A. Sridhar, P. X. Braun, et al., “Midinfrared semiconductor optical metamaterials,” *J. Appl. Phys.*, vol. 105, p. 122411, 2009.

[239] K. Feng, G. Harden, D. L. Sivco, and A. J. Hoffman, “Subdiffraction confinement in all-semiconductor hyperbolic metamaterial resonators,” *ACS Photonics*, vol. 4, p. 1621, 2017.

[240] D. Lu, H. Qian, K. Wang, et al., “Nanostructuring multilayer hyperbolic metamaterials for ultrafast and bright green InGaN quantum wells,” *Adv. Mater.*, vol. 30, p. 15, 2018.

[241] I. V. Iorsh, I. S. Mukhin, I. V. Shadrivov, P. A. Belov, and Y. S. Kivshar, “Hyperbolic metamaterials based on multilayer graphene structures,” *Phys. Rev. B*, vol. 87, p. 075416, 2013.

[242] E. E. Narimanov and A. V. Kildishev, “Naturally hyperbolic,” *Nat. Photonics*,”, vol. 9, p. 214, 2015.

[243] G. Hu, A. Krasnok, Y. Mazor, C.-W. Qiu, and A. Alù, “Moiré hyperbolic metasurfaces,” *Nano Lett.*, vol. 20, p. 3217, 2020.

[244] C. Wang, S. Huang, Q. Xing, et al., “Vander Waals thin films of WTe_2 for natural hyperbolic plasmonic surfaces,” *Nat. Commun.*, vol. 11, p. 1158, 2020.

[245] E. Itai, A. J. Chaves, D. A. Rhodes, et al., “Highly confined In-plane propagating exciton-polaritons on monolayer semiconductors,” *2D Mater.*, vol. 7, p. 3, 2020.

[246] N. Riveraa, G. Rosolen, J. D. Joannopoulosa, I. Kaminera, and M. Soljacic, “Making two-photon processes dominate one-photon processes using mid-IR phonon polaritons,” *Proc. Natl. Acad. Sci. U.S.A.*, vol. 114, p. 3607, 2017.

[247] P. A. Belov and Y. Hao, “Subwavelength imaging at optical frequencies using a transmission device formed by a periodic layered metal-dielectric structure operating in the canalization regime,” *Phys. Rev. B*, vol. 73, p. 113110, 2006.

[248] P. Li, G. Hu, I. Dolado, et al., “Collective near-field coupling and nonlocal phenomena in infrared-phononic metasurfaces for nano-light canalization,” *Nat. Commun.*, vol. 11, p. 3663, 2020.

[249] S. Dai, Q. Ma, T. Andersen, et al., “Subdiffractional focusing and guiding of polaritonic rays in a natural hyperbolic material,” *Nat. Commun.*, vol. 6, p. 6963, 2015.

[250] D. Correas-Serrano, A. Alù, and J. Sebastian Gomez-Diaz, “Plasmon canalization and tunneling over anisotropic metasurfaces,” *Phys. Rev. B*, vol. 96, p. 075436, 2017.

[251] P. Li, M. Lewin, A. V. Kretinin, et al., “Hyperbolic phonon-polaritons in boron nitride for near-field optical imaging and focusing,” *Nat. Commun.*, vol. 6, p. 7507, 2015.

[252] I.-H. Lee, M. He, X. Zhang, et al., “Image polaritons in boron nitride for extreme polariton confinement with low losses,” *Nat. Commun.*, vol. 11, p. 3649, 2020.

[253] A. Stahl, “Polariton Structure of interband Transitions in semiconductors,” *Phys. Stat. Sol.(b)*, vol. 94, p.221, 1979.

[254] A. Tomadin, F. Guinea, and M. Polini, “Generation and morphing of plasmons in graphene superlattices,” *Phys. Rev. B*, vol. 90, p. 161406, 2014.

[255] G. X. Ni, H. Wang, J. S. Wu, et al., “Plasmons in graphene moiré superlattices,” *Nat. Mater.*, vol. 14, p. 1217, 2015.

[256] N. C. H. Hesp, I. Torre, D. R-Legrian, et al., “Collective excitations in twisted bilayer graphene close to the magic angle,” arXiv:1910.07893, 2019.

[257] P. Novelli, I. Torre, F. H. L. Koppens, F. Taddei, and M. Polini, “Optical and plasmonic properties of twisted bilayer graphene: Impact of interlayer tunneling asymmetry and ground-state charge inhomogeneity,” arXiv:2005.09529, 2020.

[258] D. N. Basov, R. Liang, D. A. Bonn, et al., “In-plane anisotropy of the penetration depth in $YBa_2Cu_3O_{7-x}$ and $YBa_2Cu_4O_8$ superconductors,” *Phys. Rev. Lett.*, vol. 74, p. 598, 1995.

[259] P. A. Wolff, “Plasma-wave instability in narrow-gap semiconductors,” *Phys. Rev. Lett.*, vol. 24, p. 266, 1970.

[260] T. Low, P.-Y. Chen, and D. N. Basov “Superluminal plasmons with resonant gain in population inverted bilayer graphene” *Phys. Rev. B*, vol. 98, p. 041403(R), 2018.

[261] D. Dini, R. Kohler, A. Tredicucci, G. Biasiol, and L. Sorba, “Microcavity polariton splitting of intersubband transitions,” *Phys. Rev. Lett.*, vol. 90, p. 116401, 2003.

[262] D. Ballarini and S. D. Liberato, “Polaritonics: from microcavities to sub-wavelength confinement,” *Nanophotonics*, vol. 8, p. 641, 2019.

[263] J. Lee, M. Tymchenko, C. Argyropoulos, et al., “Giant nonlinear response from plasmonic metasurfaces Coupled to intersubband transitions,” *Nature*, vol. 511, p. 65, 2014.

[264] Y. Laplace, S. Fernandez-Pena, S. Gariglio, J. M. Triscone, and A. Cavalleri, “Proposed cavity Josephson plasmonics with complex-oxide heterostructures,” *Phys. Rev. B*, vol. 93, p. 075152, 2016.

[265] D. N. Basov and T. Timusk, “Electrodynamics of high-Tc superconductors,” *Rev. Mod. Phys.*, vol. 77, p. 721, 2005.

[266] S. Rajasekaran, E. Casandruc, Y. Laplace, et al., “Parametric amplification of a superconducting plasma wave,” *Nat. Phys.*, vol. 12, p. 1012, 2016.

[267] A. Charnukha, A. Sternbach, H. T. Stinson, et al., “Ultrafast nonlocal collective dynamics of Kane plasmon-polaritons in a narrow-gap semiconductor,” *Sci. Adv.*, vol. 5, p. eaau9956, 2019.

[268] X. Li, M. Bamba, Q. Zhang, et al., “Vacuum Bloch–Siegert shift in Landau polaritons with ultra-high cooperativity,” *Nat. Photonics*, vol. 12, p. 324, 2018.

[269] G. L. Paravicini-Bagliani, F. Appugliese, E. Richter, et al., “Magneto-transport controlled by Landau polariton states,” *Nat. Phys.*, vol. 15, p. 186, 2019.

[270] Z. Shi, X. Hong, H. A. Bechtel, et al., “Observation of a Luttinger-liquid plasmon in metallic single-walled carbon nanotubes,” *Nat. Photonics*, vol. 9, p. 515, 2015.

[271] J. M. Luttinger, “An exactly soluble model of a many-fermion system,” *J. Math. Phys.*, vol. 4, p. 1154, 1963.

[272] F. D. M. Haldane, “Luttinger liquid theory, of one-dimensional quantum fluids. I. Properties of the Luttinger model and their extension to the general 1D interacting spinless Fermi gas,” *J. Phys. C Solid State Phys.*, vol. 14, p. 2585, 1981.

[273] S. Wang, S. Zhao, Z. Shi, et al., “Nonlinear Luttinger liquid plasmons in semiconducting single-walled carbon nanotubes,” *Nat. Mater.*, vol. 19, p. 986, 2020.

[274] E. Camley, “Long-wavelength surface spin waves on antiferromagnets,” *Phys. Rev. Lett.*, vol. 45, p. 283, 1980.

[275] R. E. Camley and D. L. Millis, “Surface polaritons on uniaxial antiferromagnets,” *Phys. Rev. B*, vol. 26, p. 1280, 1982.

[276] R. Macêdo and R. E. Camley, “Engineering terahertz surface magnon-polaritons in hyperbolic antiferromagnets,” *Phys. Rev. B*, vol. 99, p. 014437, 2019.

[277] J. Sloan, N. Rivera, J. D. Joannopoulos, I. Kaminer, and M. Soljăci, “Controlling spins with surface magnon polaritons,” *Phys. Rev. B*, vol. 100, p. 235453, 2019.

[278] S. S. Kruk, Z. J. Wong, E. Pshenay-Severin, et al., “Magnetic hyperbolic optical metamaterials,” *Nat. Commun.*, vol. 7, p. 11329, 2016.

[279] P. Sivarajah, A. Steinbacher, B. Dastrup, et al., “THz-frequency magnon-phonon-polaritons in the collective strong-coupling regime,” *J. Appl. Phys.*, vol. 125, p. 213103, 2019.

[280] J. J. Brion, R. F. Wallis, A. Hartstein and E. Burstein, “Theory of surface magnetoplasmons in semiconductors,” *Phys. Rev. Lett.*, vol. 28, p. 1455, 1972.

[281] B. Hu, Y. Zhang and Q. J. Wang, “Surface magneto plasmons and their applications in the infrared frequencies,” *Nanophotonics*, vol. 4, p. 4, 2015.

[282] Z. Long, Y. Wang, M. Erukhimova, M. Tokman, and A. Belyanin, “Magnetopolaritons in Weyl semimetals in a strong magnetic field,” *Phys. Rev. Lett.*, vol. 120, p. 037403, 2018.

[283] R. L. Stamps and R. E. Camley, “Focusing of magnetoplasmon polaritons,” *Phys. Rev. B*, vol. 31, p. 4924, 1985.

[284] M. S. Rudner and J. C. W. Song, “Self-induced Berry flux and spontaneous non-equilibrium magnetism,” *Nat. Phys.*, vol. 15, p. 1017, 2019.

[285] A. K. Geim and I. V. Grigorieva, “Van der Waals heterostructures” *Nature*, vol. 499, p. 419, 2013.

[286] K. S. Novoselov, A. Mishchenko, A. Carvalho and A. H. Castro Neto, “2D materials and van der Waals heterostructures” *Science*, vol. 353, p. 6298, 2016.

[287] A. Castellanos-Gomez, “Why all the fuss about 2D semiconductors?” *Nat. Photonics*, vol. 10, p. 202, 2016.

[288] H. Schmidt, T. Ludtke, P. Barthold, E. McCann, V. I. Fal’ko and R. J. Haug, “Tunable graphene system with two decoupled monolayers,” *Appl. Phys. Lett.*, vol. 93, p. 172108, 2008.

[289] G. Li, A. Luican, J. M. B. Lopes dos Santos, et al., “Observation of Van Hove singularities in twisted graphene layers,” *Nat. Phys.*, vol. 6, p. 109, 2010.

[290] J. D. Sanchez-Yamagishi, T. Taychatanapat, K. Watanabe, T. Taniguchi, A. Yacoby and P. Jarillo-Herrero, “Quantum Hall effect, screening, and layer-polarized insulating States in twisted bilayer graphene,” *Phys. Rev. Lett.*, vol. 108, p. 076601, 2012.

[291] D. S. Lee, C. Riedl, T. Beringer, et al., “Quantum Hall effect in twisted bilayer graphene" *Phys. Rev. Lett.*, vol. 107, p. 216602, 2011.

[292] J. D. Sanchez-Yamagishi, J. Y. Luo, A. F. Young, et al., “Helical edge states and fractional quantum Hall effect in a graphene electron–hole bilayer,” *Nat. Nanotechnol.*, vol. 12, p. 118, 2017.

[293] Y. Cao, J. Y. Luo, V. Fatemi, et al., "Superlattice-induced insulating states and valley-protected orbits in twisted bilayer graphene" *Phys. Rev. Lett.*, vol. 117, p. 116804, 2016.

[294] K. Liu, L. M. Zhang, T. Cao, et al., "Evolution of interlayer coupling in twisted molybdenum disulfide bilayers," *Nat. Commun.*, vol. 5, p. 4966, 2014.

[295] M. Barbier, P. Vasilopoulos and F. M. Peeters, "Extra Dirac points in the energy spectrum for superlattices on single-layer graphene," *Phys. Rev. B*, vol. 81, p. 075438, 2010.

[296] C. R. Woods, L. Britnell, A. Eckmann, et al., "Commensurate-incommensurate transition in graphene on hexagonal boron nitride," *Nat. Phys.*, vol. 10, p. 451, 2014.

[297] B. Hunt, J. D. Sanchez-Yamagishi, A. F. Young, et al., "Massive Dirac fermions and hofstadter butterfly in a van der Waals heterostructure," *Science*, vol. 340, p. 6139, 2013.

[298] M. Yankowitz, J. Xue, D. Cormode, et al., "Emergence of superlattice Dirac points in graphene on hexagonal boron nitride," *Nat. Phys.*, vol. 8, p. 382, 2012.

[299] Y. Cao, V. Fatemi, S. Fang, et al., "Unconventional superconductivity in magic-angle graphene superlattices" *Nature*, vol. 556, p. 43, 2018.

[300] D. M. Kennes, L. Xian, M. Claassen, and A. Rubio, "One-dimensional flat bands in twisted bilayer germanium selenide," *Nat. Commun.*, vol. 11, p. 1124, 2020.

[301] L. Xian, D. M. Kennes, N. Tancogne-Dejean, M. Altarelli, and A. Rubio, "Multiflat bands and strong correlations in twisted bilayer boron nitride: doping-induced correlated insulator and superconductor," *Nano Lett.*, vol. 19, p. 4934, 2019.

[302] D. M. Kennes, M. Claassen, L. Xian, A. Georges, et al.," Moiré heterostructures: a condensed matter quantum simulator", to appear in *Nat. Phys.*, 2020.

[303] X. Chen, X. Fan, L. Li, et al., "Moiré engineering of electronic phenomena in correlated oxides," *Nat. Phys.*, vol. 16, p. 631, 2020.

[304] K. L. Seyler, P. Rivera, H. Yu, et al., "Signatures of moire-trapped valley excitons in $MoSe_2/WSe_2$ heterobilayers," *Nature*, vol. 567, p. 66, 2019.

[305] Yuan, B. Zheng, J. Kuntsmann, et al., "Twist-angle-dependent interlayer exciton diffusion in WS_2–WSe_2 heterobilayers," *Nat. Mater.*, vol. 19, p. 617, 2020.

[306] W. Li, X. Lu, S. Dubey, L. Devenica and A. Srivastava, "Dipolar interactions between localized interlayer excitons in van der Waals heterostructures," *Nat. Mater.*, vol. 19, p. 624, 2020.

[307] Y. Bai, L. Zhou, J. Wang, et al., "Excitons in strain-induced one-dimensional moire potentials at transition metal dichalcogenide heterojunctions," *Nat. Mater.*, vol. 19, p. 1068, 2020.

[308] S. S. Sunku, G. X. Ni, B. Y. Jiang, et al., "Photonic crystals for nano-light in moiré graphene superlattices" *Science*, vol. 362, p. 1153, 2018.

[309] G. X. Ni, H. Wang, B.-Y. Jiang, et al., "Soliton superlattices in twisted hexagonal boron nitride," *Nat. Commun.*, vol. 10, p. 4360, 2019.

[310] M. Chen, X. Lin, T. H. Dinh, et al., "Configurable phonon polaritons in twisted α-MoO_3," *Nat. Mater.*, 2020. https://doi.org/10.1038/s41563-020-0781-x.

[311] G. Hu, Q. Ou, G. Si, et al., "Topological polaritons and photonic magic angles in twisted α-MoO3 bilayers," *Nature*, vol. 582, p. 209, 2020.

[312] F. Herrera and J. Owrutsky, "Molecular polaritons for controlling chemistry with quantum optics," *J. Chem. Phys.*, vol. 152, p. 100902, 2020.

[313] J. P. Long and B. K. Simpkins, "Coherent coupling between a molecular vibration and Fabry–Perot optical cavity to give hybridized states in the strong coupling limit," *ACS Photonics*, vol. 2, p. 130, 2015.

[314] B. Xiang, R. F. Ribeiro, M. Du, et al., "Intermolecular vibrational energy transfer enabled by microcavity strong light–matter coupling," *Science*, vol. 368, p. 665, 2020.

[315] E. Orgiu, J. George, J. A. Hutchison, et al., "Conductivity in organic semiconductors hybridized with the vacuum field," *Nat. Mater.*, vol. 14, p. 1123, 2015.

[316] R. Chikkaraddy, B. de Nijs, F. Benz, et al., "Single-molecule strong coupling at room temperature in plasmonic nanocavities," *Nature*, vol. 535, p. 127, 2016.

[317] B. Xiang, R. F. Ribeiro, Y. Li, et al., "Manipulating optical nonlinearities of molecular polaritons by delocalization," *Sci. Adv.*, vol. 5, p. eaax5196, 2019.

[318] H. Memmi, O. Benson, S. Sadofev, and S. Kalusniak, "Strong coupling between surface plasmon polaritons and molecular vibrations," *Phys. Rev. Lett.*, vol. 118, p. 126802, 2017.

[319] L. Henriet, Z. Ristivojevic, P.P. Orth, and K. Le Hur, "Quantum dynamics of the driven and dissipative Rabi model," *Phys. Rev. A*, vol. 90, p. 023820, 2014.

[320] S. Schmidt and J. Koch, "Circuit QED lattices towards quantum simulation with superconducting circuits," *Ann. Phys. (Berlin)*, vol. 525, p. 395, 2013.

[321] M. Kiffner, J. Coulthard, F. Schlawin, A. Ardavan and D. Jaksch, "Mott polaritons in cavity-coupled quantum materials," *N. J. Phys.*, vol. 21, p. 073066, 2019.

[322] W. L. Faust and C. H. Henry, "Mixing of visible and near-resonance infrared light in GaP," *Phys. Rev. Lett.*, vol. 17, p. 1265, 1966.

[323] S. A. Holmstrom, T. Stievater, M. W. Pruessner, et al., "Guided-mode phonon-polaritons in suspended waveguides," *Phys. Rev. B*, vol. 86, p. 165120, 2012.

[324] J. D. Caldwell, L. Lindsay, V. Giannini, et al., "Low-loss, infrared and terahertz nanophotonics using surface phonon polaritons," *Nanophotonics*, vol. 4, 2015. https://doi.org/10.1515/nanoph-2014-0003.

[325] S. Vassant, F. Marquier, J. J. Greffet, F. Pardo, and J. L. Pelouard, "Tailoring GaAs terahertz radiative properties with surface phonons polaritons," *Appl. Phys. Lett.*, vol. 97, p. 161101, 2010.

[326] P. C. M. Planken, L. D. Noordam, T. M. Kermis, and A. Lagendijk, "Femtosecond time-resolved study of the generation and propagation of phonon polaritons in LiNbo," *Phys. Rev. B*, vol. 45, p.13, 1992.

[327] T. Feurer, N. S. Stoyanov, D. W. Ward, J. C. Vaughan, E. R. Statz, and K. A. Nelson, "Terahertz polaritonics," *Annu. Rev. Mater. Res.*, vol. 37, p. 317, 2007.

[328] S. Kojima, N. Tsumura and M. W. Takeda, "Far-infrared phonon-polariton dispersion probed by terahertz time-domain spectroscopy," *Phys. Rev. B*, vol. 67, p. 035102, 2003.

[329] H. J. Bakker, S. Hunsche, and H. Kurz, "Coherent phonon polaritons as probes of anharmonic phonons in ferroelectrics," *Rev. Mod. Phys.*, vol. 70, p. 2, 1998.

[330] K.-L. Yeh, M. C. Hoffman, J. Hebling, and K. A. Nelson, "Generation of 10 μJ ultrashort terahertz pulses by optical rectification," *Appl. Phys. Lett.*, vol. 90, p. 171121, 2007.

[331] A. J. Huber, N. Ocelic, and R. Hillenbrand, "Local excitation and interference of surface phonon polaritons studied by near-field infrared microscopy," *J. Microsc.*, vol. 229, p. 389, 2008.

[332] A. J. Huber, R. Hillenbrand, B. Deutsch, and L. Novotny, "Focusing of surface phonon polaritons," *Appl. Phys. Lett.*, vol. 92, p. 203104, 2008.
[333] A. A. Goyyadinov, A. Konecna, A. Chuvilin, et al., "Probing low-energy hyperbolic polaritons in van der Waals crystals with an electron microscope," *Nat. Commun.*, vol. 8, p. 95, 2017.
[334] D.-Z. A. Chen, A. Narayanaswamy, and G. Chen, "Surface phonon-polariton mediated thermal conductivity enhancement of amorphous thin films," *Phys. Rev. B*, vol. 72, p. 155435, 2005.
[335] P. S. Venkataram, J. Hermann, A. Tkatchenko, and A. W. Rodriguez, "Phonon-polariton mediated thermal radiation and heat transfer among molecules and macroscopic bodies: nonlocal electromagnetic response at mesoscopic scales," *Phys. Rev. Lett.*, vol. 121, p. 045901, 2018.
[336] D. G. Cahill, P. V. Braun, G. Chen, et al., "Nanoscale thermal transport," *Appl. Phys. Rev.*, vol. 1, p. 011305, 2014.
[337] K. Kim, B. Song, V. Fernández-Hurtado, et al., "Radiative heat transfer in the extreme near field," Nature, vol. 528, p. 387, 2015.
[338] D. Thompson, L. Zhu, R. Mittapally, et al., "Hundred-fold enhancement in far-field radiative heat transfer over the blackbody limit," *Nature*, vol. 561, p. 216, 2018.
[339] Z. Zheng, J. Chen, Y. Wang, et al., "Highly confined and tunable hyperbolic phonon Polaritons in van der waals semiconducting transition metal oxides," *Adv. Mater.*, vol. 30, p. 1705318, 2018.
[340] W. Ma, P. Alonso-Gonzalez, S. Li, et al., "In-plane anisotropic and ultra-low-loss polaritons in a natural van der Waals crystal," *Nature*, vol. 562, p. 557, 2018.
[341] Z. Zheng, N. Xu, S. L. Oscurato, et al., "A mid-infrared biaxial hyperbolic van der Waals crystal," *Sci. Adv.*, vol. 5, p. eaav8690, 2019.
[342] P. Li, I. Dolado, F. J. Alfaro-Mozaz, et al., "Infrared hyperbolic metasurface based on nanostructured van der Waals materials," *Science*, vol. 359, p. 892, 2018.
[343] A. Cartella, T. F. Nova, M. Fechner, R. Merlin, and A. Cavalleri, "Parametric amplification of optical phonons," *Proc. Natl. Acad. Sci. U.S.A.*, vol. 115, p. 12148, 2018.
[344] S. Dai, F. Wenjing, N. Rivera, et al., "Phonon polaritons in monolayers of hexagonal boron nitride" *Adv. Mater.*, vol. 31, p. 1806603, 2019.
[345] A. V. Zayats, I. I. Smolyaninov and A. A. Maradudin, "Nano-optics of surface plasmon polaritons," *Phys. Rep.*, vol. 408, p. 131, 2005.
[346] S. A. Maier, *Plasmonics: Fundamentals and Applications*, Berlin, Springer, 2007.
[347] D. K. Gramotney and S. I. Bozhevolnvi, "Plasmonics beyond the diffraction limit," *Nat. Photonics*, vol. 4, p. 83, 2010.
[348] H. A. Atwater and A. Polman, "Plasmonics for improved photovoltaic devices," *Nat. Mater.*, vol. 9, p. 205, 2010.
[349] P. Berini and I. De Leon, "Surface plasmon-polariton amplifiers and lasers," *Nat. Photonics*, vol. 6, p. 16, 2012.
[350] S. I. Bogdanov, A. Boltasseva, and V. M. Shalev, "Overcoming quantum decoherence with plasmonics," *Science*, vol. 364, p. 532, 2019.
[351] J. Lee, S. Jung, P. Y. Chen, et al., "Ultrafast electrically-tunable polaritonic metasurfaces," *Adv. Opt. Mater.*, vol. 2, p. 1057, 2014.
[352] M. Kauranen and A. V. Zayats, "Nonlinear plasmonics," *Nat. Photonics*, vol. 6, p. 73, 2012.
[353] J. Lee, N. Nookala, J. S. Gomez-Diaz, et al., "Ultrathin gradient nonlinear metasurfaces with giant nonlinear response," *Optica*, vol. 3, p. 283, 2016.
[354] M. Tymchenko, J. S. Gomez-Diaz, J. Lee, M. A. Belkin, and A. Alù, "Gradient nonlinear Pancharatnam–Berry metasurfaces," *Phys. Rev. Lett.*, vol. 115, p. 207403, 2015.
[355] Z. Jacob, and V. M. Shalev, "Plasmonics goes quantum," *Science*, vol. 334, p. 463, 2011.
[356] M. S. Tame, K. R. McEnery, S. K. Ozdemir, J. Lee, S. A. Maier, and M. S. Kim, "Quantum plasmonics," *Nat. Phys.*, vol. 9, p. 329, 2013.
[357] S. I. Bozhevolnvi and J. B. Khurgin, "The case for quantum plasmonics," *Nat. Photonics*, vol. 11, p. 398, 2017.
[358] J. S. Fakonas, A. Mitskovets, and H. A. Atwater, "Path entanglement of surface plasmons," *New J. Phys.*, vol. 17, p. 023002, 2015.
[359] M.-C. Dheur, F. Devaux, T. W. Ebbesen, et al., "Single-plasmon interferences," *Sci. Adv.*, vol. 2, p. e1501574, 2016.
[360] M. Wagner, A. S. McLeod, S. J. Maddox, et al., "Ultrafast dynamics of surface plasmons in InAs by time-resolved infrared nanospectroscopy," *Nano Lett.*, vol. 14, p. 4529, 2014.
[361] K. F. MacDonald, Z. L. Samson, M. I. Stockman and N. I. Zheludev, "Ultrafast active plasmonics," *Nat. Photonics*, vol. 3, p. 55, 2009.
[362] M. Eisele, T. L. Cocker, M. A. Huber, et al., "Ultrafast multi-terahertz nano-spectroscopy with sub-cycle temporal resolution," *Nat. Photonics*, vol. 8, p. 841, 2014.
[363] M. A. Huber, F. Mooshammer, M. Plankl, et al., "Femtosecond photo-switching of interface polaritons in black phosphorus heterostructures," *Nat. Nanotechnol.*, vol. 12, p. 207, 2017.
[364] Z. Yao, S. Xu, D. Hu, X. Chen, Q. Dai, and M. Liu, "Nanoimaging and nanospectroscopy of polaritons with time resolved s-SNOM," *Adv. Opt. Mater.*, vol. 8, p. 1901042, 2020.
[365] A V Krasavin, A. V. Zayats and N. I. Zheludev, "Active control of surface plasmon-polariton waves," *J. Opt. Pure Appl. Opt.*, vol. 7, p. S85, 2005.
[366] J. Shi, M. H. Lin, I. T. Chen, et al., "Cascaded exciton energy transfer in a monolayer semiconductor lateral heterostructure assisted by surface plasmon polariton," *Nat. Commun.*, vol. 8, p. 35, 2017.
[367] B. Min, E. Ostby, V. Sorger, et al., "High-Q surface-plasmon-polariton whispering-gallery microcavity," *Nature*, vol. 457, p. 455, 2009.
[368] A. Boltasseva and H. A. Atwater, "Low-loss plasmonic metamaterials," *Science*, vol. 331, p. 290, 2011.
[369] G. V. Naik and V. M. Shalaev, "Alternative plasmonic materials: beyond gold and silver," *Adv. Mater.*, vol. 25, p. 3264, 2013.
[370] F. Xia, H. Wang, D. Xiao, M. Dubey, and A. Ramasubramaniam, "Two-dimensional material nanophotonics," *Nat. Photonics*, vol. 8, p. 899, 2014.
[371] F. H. da Jornada, L. Xian, A. Rubio, and S. G. Louie, "Universal slow plasmons and giant field enhancement in atomically thin quasi-twodimensional metals," *Nat. Commun.*, vol. 11, p. 1013, 2020.
[372] E. H. Hwang and S. Das Sarma, "Plasmon modes of spatially separated doublelayer graphene," *Phys. Rev. B*, vol. 80, p. 205405, 2009.
[373] A. Principi, R. Asgari, and M. Polini, "Acoustic plasmons and composite hole-acoustic plasmon satellite bands in graphene on a metal gate," *Solid State Commun.*, vol. 151, p. 1627, 2011.
[374] R. E. V. Profumo, R. Asgari, M. Polini, and A. H. MacDonald, "Double-layer graphene and topological insulator thin-film plasmons," *Phys. Rev. B*, vol. 85, p. 085443, 2012.

[375] S. Chen, M. Autore, J. Li, P. Li, et al., “Acoustic graphene plasmon nanoresonators for field-enhanced infrared molecular spectroscopy,” *ACS Photonics*, vol. 4, p. 3089, 2017.

[376] T. Stauber and G. Gomez-Santos, “Plasmons in layered structures including graphene,” *New J. Phys.*, vol. 14, p. 105018, 2012.

[377] I.-H. Lee, D. Yoo, P. Avouris, T. Low and S.-H. Oh, “Graphene acoustic plasmon resonator for ultrasensitive infrared spectroscopy, “*Nat. Nanotechnol.*, vol. 14, p. 313, 2019.

[378] P. Alonso-Gonzalez, A. Y. Nikitin, Y. Gao, et al., “Acoustic terahertz graphene plasmons revealed by photocurrent nanoscopy,” *Nat. Nanotechnol.*, vol. 12, p. 31, 2017.

[379] M. B. Lundeberg, Y. Gao, R. Asgari, et al., “Tuning quantum nonlocal effects in graphene plasmonics,” *Science*, vol. 347, p. 187, 2017.

[380] J. B. Pendry, L. Martin-Moreno, and F. J. Garcia-Vidal, “Mimicking surface plasmons with structured surfaces,” *Science*, vol. 305, p. 847, 2014.

[381] M. V. Berry and N. L. Balazs, “Nonspreading wave packets,” *Am. J. Phys.*, vol. 47, p. 264, 1979.

[382] A. Minovich, A. E. Klein, N. Janunts, T. Pertsch, D. N. Neshev, and Y. S. Kivshar, “Generation and near-field Imaging of airy surface plasmons,” *Phys. Rev. Lett.*, vol. 107, p. 116802, 2011.

[383] M. Hentschel, M. Schäferling, X. Duan, H. Giessen, N. Liu, “Chiral plasmonics,” *Sci. Adv.*, vol. 3, p. e1602735, 2017.

[384] T. Stauber, T. Low, and G. Gómez-Santos, “Chiral response of twisted bilayer graphene,”*Phys. Rev. Lett.*, vol. 120, p. 046801, 2018.

[385] D. N. Basov and M. M. Fogler, “Quantum Materials: The quest for ultrafast plasmonics,” *Nat. Nanotechnol.*, vol. 12, p. 187, 2017.

[386] P. Vasa, W. Wang, R. Pomraenke, et al., “Real-time observation of ultrafast Rabi oscillations between excitons and plasmons in metal nanostructures with J-aggregates,” *Nat. Photonics*, vol. 7, p. 128, 2013.

[387] N. T. Fofang, T. H. Park, O. Neumann, N. A. Mirin, P. Nordlander and N. J. Halas, “Plexcitonic nanoparticles: plasmon-exciton coupling in nanoshell-J-aggregate complexes,” *Nano Lett.*, vol. 8, p. 3481, 2008.

[388] N. T. Fofang, N. K. Grady, Z. Fan, A. O. Govorov, and N. J. Halas, “Plexciton dynamics: exciton-plasmon coupling in a J-aggregate–Au nanoshell complex provides a mechanism for nonlinearity,” *Nano Lett.*, vol. 11, p. 1556, 2011.

[389] A. Manjavacas, F. J. Garcia de Abajo and P. Nordlander, “Quantum plexcitonics: strongly interacting plasmons and excitons,” *Nano Lett.*, vol. 11, p. 2318, 2011.

[390] J. Yuen-Zhou, S. K. Saikin, T. Zhu, et al., “Plexciton Dirac points and topological modes,” *Nat. Commun.*, vol. 7, p. 11783, 2016.

[391] A. P. Manuel, A. Kirkey, N. Mahdi and K. Shankar, “Plexcitonics – fundamental principles and optoelectronic applications,” *J. Mater. Chem. C*, vol. 7, 2019. https://doi.org/10.1039/c8tc05054f.

[392] K. Wu, W. E. Rodriguez-Cordoba, Y. Yang, and T. Lian, “Plasmon-induced hot electron transfer from the Au tip to CdS rod in CdS-Au nanoheterostructures,” *Nano Lett.*, vol. 13, p. 5255, 2013.

[393] P. Torma and W. L. Barnes, “Strong coupling between surface plasmon polaritons and emitters: a review,” *Rep. Prog. Phys.*, vol. 78, p. 013901, 2015.

[394] P. A. D. Goncalves, L. P. Bertelsen, S. Xiao and N. Mortensen, “Plasmon-exciton polaritons in two-dimensional semiconductor/metal interfaces,” *Phys. Rev. B*, vol. 97, p. 041402, 2018.

[395] V. Karanikolas, I. Thanopulos, and E. Paspalakis, “Strong interaction of quantum emitters with a WS_2 layer enhanced by a gold substrate,” *Opt. Lett.*, vol. 44, p. 2049, 2019.

[396] T. Chervy, S. Azzini, E. Lorchat, et al., “Room temperature chiral coupling of valley excitons with spin-momentum locked surface plasmons” *ACS Photonics*, vol. 5, p. 1281, 2018.

[397] H. Groß, J. M. Hamm, T. Tufarelli, O. Hess, and B. Hecht, “Near-field strong coupling of single quantum dots,” *Sci. Adv.*, vol. 4, p. eaar4906, 2018.

[398] M. A. May, D. Fialkow, T. Wu, et al., “Nano-cavity QED with tunable nano-tip interaction,” *Adv. Quantum Technol.*, vol. 3, p. 190087, 2020.

[399] M. Saba, C. Ciuti, J. Bloch, et al., “High-temperature ultrafast polariton parametric amplification in semiconductor microcavities,” *Nature*, vol. 414, p. 731, 2001.

[400] S. Kéna-Cohen and S. R. Forrest, “Room-temperature polariton lasing in an organic single-crystal microcavity,” *Nat. Photonics*, vol. 4, p. 371, 2010.

[401] H. Deng, G. Weihs, D. Snoke, J. Bloch, and Y. Yamamoto, “Polariton lasing vs. photon lasing in a semiconductor microcavity,” *Proc. Natl. Acad. Sci. U.S.A.*, vol. 23, p. 5318, 2003.

[402] Y. Liu, H. Fang, A. Rasmita, et al., “Room temperature nanocavity laser with interlayer excitons in 2D heterostructures,” *Sci. Adv.*, vol. 5, p. eaav4506, 2019.

[403] J. Flick, N. Rivera and P. Narang, “Strong light–matter coupling in quantum chemistry and quantum photonics,” *Nanophotonics*, vol. 7, p. 1479, 2018.

[404] J. A. Hutchison, T. Schwartz, C. Genet, E. Devaux, and T. W. Ebbesen, “Modifying chemical landscapes by coupling to vacuum fields,” *Angew. Chem. Int. Ed.*, vol. 51, p. 1592, 2012.

[405] J. Yuen-Zhou and V. M. Menon, “Polariton chemistry: thinking inside the (photon) box,” *Proc. Natl. Acad. Sci. U.S.A.*, vol. 116, p. 5214, 2019.

[406] J. Flick, M. Ruggenthaler, H. Appel, and A. Rubio “Atoms and molecules in cavities: from weak to strong coupling in QED chemistry,” *Proc. Natl. Acad. Sci. U.S.A.*, vol. 114, p. 3026, 2017.

[407] C. Schäfer, M. Ruggenthaler, V. Rokaj, and A. Rubio, “Relevance of the quadratic diamagnetic and self-polarization terms in cavity quantum electrodynamics,” *ACS Photonics*, vol. 7, p. 975, 2020.

[408] D. Sanvitto and S. Kéna-Cohen, “The road towards polaritonic devices,” *Nat. Mater.*, vol. 15, p. 1061, 2016.

[409] A. Amo, T. C. H. Liew, C. Adrados, et al., “Exciton-polariton spin switches,” *Nat. Photonics*, vol. 4, p. 361, 2010.

[410] T. Gao, P. Eldridge, T. Liew, et al., “Polariton condensate transistor switch,” *Phys. Rev. B*, vol. 85, p. 235102, 2012.

[411] D. Ballarini, M. De Giorgi, E. Cancellieri, et al., “All-optiocal polariton transistor,” *Nat. Commun.*, vol. 4, p. 1778, 2013.

[412] C. Antón, T. C. H. Liew, J. Cuadra, et al., “Quantum refelctions and shunting of polariton condensate wave trains: Implementation of a logic AND gate,” *Phys. Rev. B*, vol. 88, p. 245307, 2013.

[413] H. S. Nguyen, D. Vishnevsky, C. Sturm, et al., "Realization of a double-barrier resonant tunneling Diode for cavity polaritons," *Phys. Rev. Lett.*, vol. 110, p. 236601, 2013.
[414] F. Marsault, H. S. Nguuyen, D. Tanese, et al., "Realization of an all optical exciton-polariton router," *Appl. Phys. Lett.*, vol. 107, p. 201115, 2015.
[415] A. Kavokin, T. C. H. Liew, C. Schneider, S. Hofling "Bosonic lasers" *Low Temp. Phys.*, vol. 42, p. 323, 2016.
[416] D. Ballarini, A. Gianfrate, R. Panico, et al., "Polaritonic neuromorphic computing outperforms linear classifiers," *Nano Lett.*, vol. 20, p. 3506, 2020.
[417] J. Gu, B. Chakraborty, M. Khatoniar and V. M. Menon, "A room-temperature polariton light-emitting diode based on monolayer WS2," *Nat. Nanotechnol.*, vol. 14, p. 1024, 2019.
[418] E. A. Cerda-Méndez, D. N. Krizhanovskii, M. Wouters, et al., "Polariton Condensation in dynamic acoustic lattices," *Phys. Rev. Lett.*, vol. 105, p. 116402, 2010.
[419] A. Amo and J. Bloch, "Exciton-polaritons in lattices: a non-linear photonic simulator," *Compt. Rendus Phys.*, vol. 17, p. 934, 2016.
[420] L. Zhang, W. Xie, J. Wang, et al., "Weak lasing in one-dimensional polariton superlattices," *Proc. Natl. Acad. Sci. U.S.A.*, vol. 112, p. E1516, 2015.
[421] M. J. Hartmann, F. G. S. L. Brandao, and M. B. Plenio, "Quantum many-body phenomena in coupled cavity arrays," *Laser Photonics*, vol. 2, p. 6, 2008.
[422] N. Y. Kim and Y. Yamamoto, "*Exciton-Polariton Quantum Simulators in Quantum Simulations with Photons and Polaritons*," vol. 91, D. Angelakis, ed., Springer, 2017.
[423] I. M. Georgescu, S. Ashhab and F. Nori, "Quantum simulation," *Rev. Mod. Phys.*, vol. 86, p. 153, 2014.
[424] J. I. Cirac and P. Zoller, "Golas and opportunities in quantum simulation," *Nat. Phys.*, vol. 8, p. 264, 2012.
[425] I. Bloch, J. Dalibard, and S. Nascimbene, "Quantum simulations with ultracold quantum gases," *Nat. Phys.*, vol. 8, p. 267, 2012.
[426] N. C. Harris, G. R. Steinbrecher, M. Prabhu, et al., "Quantum transport simulations in a programmable nanophotonic processor," *Nat. Photonics*, vol. 11, p. 447, 2017.
[427] A. Aspuru-Guzik and P. Walther, "Photonic quantum simulators," *Nat. Phys.*, vol. 8, p. 285, 2012.
[428] M. J. Hartmann, F. G. S. L. Brandao, and M. B. Plenio, "Strongly interacting polaritons in coupled arrays of cavities," *Nat. Phys.*, vol. 2, p. 849, 2006.
[429] A. D. Greentree, C. Tahan, J. H. Cole, and L. C. L. Hollenberg, "Quantum phase transitions of light," *Nat. Phys.*, vol. 2, p. 856, 2006.
[430] T. Byrnes, P. Recher, and Y. Yamamoto, "Mott transitions of excitons polaritons and indirect excitons in a periodic potential," *Phys. Rev. B*, vol. 81, p. 205312, 2010.
[431] N. Na and Y. Yamamoto, "Massive parallel generation of indistinguishable single photons iva the polaritonic superfluid to Mott-insulator quantum phase transition," *New J. Phys.*, vol. 12, p. 123001, 2010.
[432] N. G. Berlo, M. Silva, K. Kalinin, et al., "Realizing the classical XY Hamiltonian in polariton simulators," *Nat. Mater.*, vol. 16, p. 1120, 2017.
[433] T. Esslinger, "Fermi-hubbard Physics with Atoms in an optical lattice," *Ann. Rev. Condensed Matter Phys.*, vol. 1, p. 129, 2010.
[434] R. Blatt and C. F. Roos, "Quantum simulations with trapped ions," *Nat. Phys.*, vol. 8, p. 277, 2012.
[435] K. Kim, S. Korenblit, R. Islam, et al., "Quantum simulation of the transverse Ising model with trapped ions," *New J. Phys.*, vol. 13, p. 105003, 2011.
[436] J. W. Britton, B. C. Sawyer, A. C. Keith, et al., "Engineered two-dimensional Ising interactions in a trapped-ion quantum simulator with hundreds of spins," *Nature*, vol. 484, p. 489, 2012.
[437] A. A. Houck, H. Tureci, and J. Koch, "On-chip quantum simulation with superconducting circuits," *Nat. Phys.*, vol. 8, p. 292, 2012.
[438] J. Koch, A. A. Houck, K. Le Hur, and S. M. Girvin, "Time-reversal-symmetry breaking in circuit-QED-based photon lattices," *Phys. Rev. A*, vol. 82, p. 043811, 2010.
[439] L. Xiong, C. Forsythe, M. Jung, et al., "Photonic crystal for graphene plasmons" *Nat. Commun.*, vol. 10, p. 4780, 2019.
[440] B.-Y. Jiang, G.-X. Ni, Z. Addison, et al., "Plasmon reflections by topological electronic boundaries in bilayer graphene," *Nano Lett.*, vol. 17, p. 7080, 2017.
[441] Z. Fei, G. X. Ni, B. Y. Jiang, M. M. Fogler, and D. N. Basov, "Nanoplasmonic phenomena at electronic boundaries in graphene," *ACS Photonics*, vol. 4, no. 12, p. 2971, 2017.
[442] J. Chen, M. L. Nesterov, A. Y. Nikitin, et al., "Strong plasmon reflection at nanometer-size gaps in monolayer graphene on SiC," *Nano Lett.*, vol. 13, p. 6210, 2013.
[443] E. H. Hasdeo and J. C. W. Song, "Long-lived domain wall plasmons in gapped bilayer graphene," *Nano Lett.*, vol. 17, p. 7252, 2017.
[444] R. Zia and M. L. Brongersma, "Surface plasmon polariton analogue to Young's double-slit experiment," *Nat. Nanotechnol.*, vol. 2, p. 426, 2007.
[445] P. Li, M. Lewin, A. V. Kretinin, et al., "Hyperbolic phonon-polaritons in boron nitride for near-field optical imaging and focusing," *Nat. Commun.*, vol. 7, p. 7507, 2015.
[446] C. Yang, Q. Wu, J. Xu, K. A. Nelson, and C. A. Werley, "Experimental and theoretical analysis of THz-frequency, direction-dependent, phonon polariton modes in a subwavelength, anisotropic slab waveguide," *Opt. Express*, vol. 18, p. 26351, 2010.
[447] P. Peier, K. A. Nelson and T. Feurer, "Coherent phase contrast imaging of THz phonon-polariton tunneling," *Appl. Phys. B*, vol. 99, p. 433, 2010.
[448] J. Lin, J. Dellinger, P. Genevet, B. Cluzel, F. Fornel, and F. Capasso, "Cosine-gauss plasmon beam: a localized long-range nondiffracting surface wave," *Phys. Rev. Lett.*, vol. 109, p. 093904, 2012.
[449] I. Epstein and A. Arie, "Arbitrary bending plasmonic light waves," *Phys. Rev. Lett.*, vol. 112, p. 023903, 2014.
[450] A. R. Davoyan, I. V. Shadrivov, and Y. S. Kivshar, "Self-focusing and spatial plasmon-polariton solitons," *Opt. Express*, vol. 17, p. 21732, 2009.
[451] J. Levinsen, G. Li, and M. M. Parish, "Microscopic description of exciton-polaritons in microcavities," *Phys. Rev. Res.*, vol. 1, p. 033120, 2019.
[452] L. Nguyen-thˆe, S. De Liberato, M. Bamba, and C. Ciuti, "Effective polariton-polariton interactions of cavity-embedded two-dimensional electron gases," *Phys. Rev. B*, vol. 87, p. 235322, 2013.
[453] Y. S. Yoseob Yoon, M. Steger, G. Liu, et al., "Direct measurement of polariton–polariton interaction strength," *Nat. Phys.*, vol. 13, p. 870, 2017.

[454] E. Estrecho, T. Gao, N. Bobrovska, et al., "Direct measurement of polariton-polariton interaction strength in the Thomas–Fermi regime of exciton-polariton condensation," *Phys. Rev. B*, p. 035306, 2019.
[455] X. Lina, Y. Yangc, N. Riverab, et al., "All-angle negative refraction of highly squeezed plasmon and phonon polaritons in graphene–boron nitride heterostructures," *Proc. Natl. Acad. Sci. U.S.A.*, vol. 114, p. 6717, 2017.
[456] K. Chaudhary, M. Tamagnone, X. Yin, et al., "Polariton nanophotonics using phase-change materials," *Nat. Commun.*, vol. 10, p. 4487, 2019.
[457] P. Alonso-González, A. Y. Nikitin, F. Golmar, et al., "Controlling graphene plasmons with resonant metal antennas and spatial conductivity patterns," *Science*, vol. 344, p. 1369, 2014.
[458] M. Sidler, P. Back, O. Cotlet, et al., "Fermi polaron-polaritons in charge-tunable atomically thin semiconductors," *Nat. Phys.*, vol. 13, p. 255, 2017.
[459] D. K. Efimkin and A. H. MacDonald, "Many-body theory of trion absorption Features in two-dimensional semiconductors," *Phys. Rev. B*, vol. 95, p. 035417, 2017.
[460] G. Scalari, C. Maissen, D. Turcinkova, et al., "Ultrastrong coupling of the cyclotron transition of a 2D electron gas to a THz metamaterial," *Science*, vol. 335, p. 1323, 2012.
[461] F. M. D. Pellegrino, V. Giocannetti, A. H. MacDonald, and M. Polini, "Modulated phases of graphene quantum Hall polariton fluids," *Nat. Commun.*, vol. 7, p. 13355, 2016.
[462] I. Neder, N. Ofek, Y. Chung, M. Heiblum, D. Mahalu, and V. Umansky, "Interference between two indistinguishable electrons from independent sources," *Nature (London)*, vol. 448, p. 333, 2007.
[463] C. Bäuerle, D. C. Glattli, T. Meunier, et al., "Coherent control of single electrons: a review of current progress," *Rep. Prog. Phys.*, vol. 81, p. 056503, 2018.
[464] J. Splettstoesser and R. J. Haug, "Single-electron control in solid state devices," *Phys. Status Solidi*, vol. B254, p. 1770217, 2017.
[465] D. C. Glattli and P. S. Roulleau, "Levitons for electron quantum optics," *Phys. Status Solidi*, vol. B254, p. 1600650, 2016.
[466] S. Smolka, W. Wuester, F. Haupt, S. Faelt, W. Wegscheider, and A. Imamoglu, "Cavity quantum electrodynamics with many-body states of a two-dimensional electron gas," *Science*, vol. 346, p. 332, 2014.
[467] P. Knuppel, S. Ravets, M. Kroner, S. Falt, W. Wegscheider, and A. Imamoglu, "Nonlinear optics in the fractional quantum Hall regime," *Nature*, vol. 572, p. 91, 2019.
[468] L. Bing Tan, O. Cotlet, A. Bergschneider, et al., "Interacting polaron-polaritons," *Phys. Rev. X*, vol. 10, p. 021011, 2020.
[469] M. Sich, L. E. Tapia-Rodriguez, H. Sigurdsson, et al., "Spin domains in one-dimensional conservative polariton solitons," *ACS Photonics*, vol. 5, p. 5095, 2018.
[470] M. D. Lukin, M. Fleischhauer, R. Cote, et al., "Dipole Blockade and quantum information Processing in mesoscopic atomic ensembles," *Phys. Rev. Lett.*, vol. 87, p. 037901, 2001.
[471] D. Comparat and P. Pillet, "Dipole blockade in a cold Rydberg atomic sample," *J. Opt. Soc. Am. B*, vol. 27, p. A208, 2010.
[472] A. V. Gorshkov, J. Otterbach, M. Fleischhauer, T. Pohl, and M. D. Lukin, "Photon–photon interactions via Rydberg blockade," *Phys. Rev. Lett.*, vol. 107, p. 133602, 2011.
[473] E. Shahmoon, G. Kurizki, M. Fleischhauer, and D. Petrosyan, "Strongly interacting photons in hollow-core waveguides," *Phys. Rev. A*, vol. 83, p. 033806, 2011.
[474] T. Peyronel, O. Firstenberg, Q.-Y. Liang, et al., "Quantum nonlinear optics with single photons enabled by strongly interacting atoms," *Nature*, vol. 488, p. 57, 2012.
[475] A. Chernikov, T. C. Berkelbach, H. M. Hill, et al., "Exciton binding energy and nonhydrogenic Rydberg series in monolayer WS_2," *Phys. Rev. Lett.*, vol. 113, p. 076802, 2014.
[476] P. Merkl, F. Mooshammer, S. Brem, et al., "Twist-tailoring Coulomb correlations in van der Waals homobilayers," *Nat. Commun.*, vol. 11, p. 2167, 2020.
[477] T. Kazimierczuk, D. Fröhlich, S. Scheel, H. Stolz, and M. Bayer, "Giant Rydberg excitons in the copper oxide Cu_2O," *Nature*, vol. 514, p. 343, 2014.
[478] W. P. Su, J. R. Schrieffer, and A. J. Heeger, "Solitons in polyacetylene," *Phys. Rev. Lett.*, vol. 42, p. 1698, 1979.
[479] P. St-Jean, V. Goblot, E. Galopin, et al., "Lasing in topological edge states of a one-dimensional lattice," *Nat. Photonics*, vol. 11, p. 651, 2017.
[480] M. Bello, G. Platero, J. I. Cirac, and A. González-Tudela Bello, "Unconventional quantum optics in topological waveguide QED," *Sci. Adv.*, vol. 5, p. eaaw0297, 2019.
[481] C. A. Downing, T. J. Sturges, G. Weick, M. Stobinska, and L. Martin-Moreno, "Topological phases of polaritons in a cavity waveguide," *Phys. Rev. Lett.*, vol. 123, p. 217401, 2019.
[482] A. Bhattacharya, M. Zunaid Baten, I. Iorsh, T. Frost, A. Kavokin, and P. Bhattacharya, "Room-temperature spin polariton diode laser," *Phys. Rev. Lett.*, vol. 119, p. 067701, 2017.
[483] A. Agarwal, M. Polini, G. Vignale, and M. E. Flatt, "Long-lived spin plasmons in a spin-polarized two-dimensional electron gas," *Phys. Rev. B*, vol. 90, p. 155409, 2014.
[484] L. I. Magarill, A. V. Chaplik, and M. V. Éntin, "Spin-plasmon oscillations of the two-dimensional electron gas," *J. Exp. Theor. Phys.*, vol. 92, p. 15, 2001.
[485] S. Raghu, S. Bum Chung, X. L. Qi, and S.-C. Zhang, "Collective Modes of a helical liquid," *Phys. Rev. Lett.*, vol. 104, p. 116401, 2010.
[486] J. B. Pendry, D. Schurig, and D. R. Smith, "Controlling electromagnetic electromagnetic fields," *Science*, vol. 312, p. 1780, 2006.
[487] Ulf Leonhardt, "Optical conformal mapping," *Science*, vol. 312, p. 1777, 2006.
[488] P. A. Huidobro, M. L. Nesterov, L. Martın-Moreno, and F. J. Garcıa, "Vidal transformation optics for plasmonics," *Nano Lett.*, vol. 10, p. 1985, 2010.
[489] V. Ginis, P. Tassin, J. Danckaert, C. M. Soukoulis and I. Veretennicoff, "Creating electromagnetic cavities using transformation optics," *New J. Phys.*, vol. 14, p. 03300, 2012.
[490] A. Vakil and N. Engheta, "Transformation optics using graphene," *Science*, vol. 332, p. 1291, 2011.
[491] I. Tamm, "Über eine mögliche Art der Elektronenbindung an Kristalloberflächen," *Z. Phys.*, vol. 76, p. 849, 1932.
[492] M. Kaliteevski, I. Iorsh, S. Brand, et al., "Tamm plasmon-polaritons: possible electromagnetic states at the interface of a metal and a dielectric Bragg mirror," *Phys. Rev. B*, vol. 76, p. 165415, 2007.
[493] B. Liu, R. Wu, and V. M. Menon, "Propagating hybrid Tamm exciton Polaritons in organic microcavity," *J. Phys. Chem. C*, vol. 123, no. 43, p. 26509, 2019.

[494] S. Dhara, C. Chakraborty, K. M. Goodfellow, et al., “Anomalous dispersion of microcavity trion-polaritons,” *Nat. Phys.*, vol. 14, p. 130, 2017.

[495] R. P. A. Emmanuele, M. Sich, O. Kyriienko, et al., “Highly nonlinear trion-polaritons in a monolayer semiconductor,” *Nat. Commun.*, vol. 11, p. 3589, 2020.

[496] C. Möhl, A. Graf, F. J. Berger, et al., “Trion-polariton formation in single-walled carbon nanotube microcavities,” *ACS Photonics*, vol. 5, p. 2074, 2018.

[497] S. de Vega and F. Javier García de Abajo, “Plasmon generation through electron tunneling in graphene,” *ACS Photonics*, vol. 4, p. 2367, 2017.

[498] A. Woessner, A. Misra, Y. Cao, et al., “Propagating plasmons in a charge-neutral quantum tunneling transistor,” *ACS Photonics*, vol. 4, p. 3012, 2017.

[499] X. Xu, W. Yao, D. Xiao, and T. Heinz, “Spin and pseudospins in layered transition metal dichalcogenides,” *Nat. Phys.*, vol. 10, p. 343, 2014.

[500] R. Peng, C. Wu, H. Li, X. Xu, and M. Li, “Separation of the valley exciton-polariton in two-dimensional semiconductors with an anisotropic photonic crystal,” *Phys. Rev. B*, vol. 101, p. 245418, 2020.

[501] S. Guddala, R. Bushati, M. Li, A. B. Khanikaev, and V. M. Menon, “Valley selective optical control of excitons in 2D semiconductors using a chiral metasurface,” *Opt. Mater. Express*, vol. 9, p. 536, 2019.

[502] I. Egri and A. Stahl, “Real space wave equation for exciton-polaritons pf wannier type,” *Phys. Status Solidi*, vol. 96, p. K83, 1979.

[503] G. Calajo, F. Ciccarello, D. Chang, and P. Rabl, “Atom-field dressed states in slow-light waveguide QED,” *Phys. Rev. A*, vol. 93, p. 033833, 2016.

[504] B. K. Ofori-Okai, P. Sivarajah, C. A. Werley, S. M. Teo, and K. A. Nelson, “Direct experimental visualization of waves and band structure in 2D photonic crystal slabs,” *New J. Phys.*, vol. 16, p. 053003, 2014.

[505] A. Asenjo-Garcia, J. D. Hood, D. E. Chang, and H. J. Kimble, “Atom-light interactions in quasi-one-dimensional nanostructures: a Green’s-function perspective,” *Phys. Rev. A*, vol. 95, p. 033818, 2017.

[506] E. Vetsch, D. Reitz, G. Sagué, R. Schmidt, S. T. Dawkins, and A. Rauschenbeutel, “Optical interface created by laser-cooled atoms trapped in the evanescent field surrounding an optical nanofiber,” *Phys. Rev. Lett.*, vol. 104, p. 203603, 2010.

[507] A. Goban, K. S. Choi, D. J. Alton, et al., “Demonstration of a state-insensitive, compensated nanofiber trap,” *Phys. Rev. Lett.*, vol. 109, p. 033603, 2012.

[508] A. Goban, C.-L. Hung, J. D. Hood, et al., “Superradiance for atoms trapped along a photonic crystal waveguide,” *Phys. Rev. Lett.*, vol. 115, p. 063601, 2015.

[509] J. D. Hood, A. Goban, A. Asenjo-Garcia, et al., “Atom–atom interactions around the band edge of a photonic crystal waveguide,” *Proc. Natl. Acad. Sci. U.S.A.*, vol. 113, p. 10507, 2016.

[510] M. Mirhosseini, E. Kim, X. Zhang, et al., “Cavity quantum electrodynamics with atom-like mirrors,” *Nature*, vol. 569, p. 692, 2019.

[511] Y. Liu and A. A. Houck, “Quantum electrodynamics near a photonic bandgap,” *Nat. Phys.*, vol. 13, p. 48, 2017.

[512] T. Shi, Y.-H. Wu, A. González-Tudela, and J. I. Cirac, “Bound states in boson impurity models,” *Phys. Rev. X*, vol. 6, p. 021027, 2016.

[513] J. Zenneck, “Fortplfanzung ebener elektromagnetischer Wellenlängs einer ebenen Leiterfläche,” *Ann. Phys.*, vol. 328, p. 846, 1907.

[514] K. A. Norton, “Propagation of radio waves over the surface of the earth and in the upper atmosphere,” *Proc. IRE*, vol. 24, p. 1367, 1936.

[515] A. Sommerfeld, “Uber die Ausbreitung der Wellen in derdrahtlosen Telegraphie,”*Ann. Phys.*, vol. 333, p. 665, 1909.

[516] M. Sarrazin and J.-P. Vigneron, “Light transmission assisted by Brewster–Zennek modes in chromium films carrying a subwavelength hole array,” *Phys. Rev. B*, vol. 71, p. 075404, 2005.

[517] A. Shivola, J. Qi, and I. V. Lindell, “Bridging the gap between plasmonics and Zenneck waves,” *IEEE Antenn. Propag. Mag.*, vol. 52, p. 124, 2010.

[518] K. A. Michalski and J. R. Mosig, “The sommerfeld halfspace problem redux: alternative field representations, Role of Zenneck and surface plasmon waves,” *IEEE Trans. Antenn. Propag.*, vol. 63, 2015. https://doi.org/10.1109/tap.2015.2489680.

[519] A. Yu Nikitin, S. G. Rodrigo, F. J. García-Vidal and L. Martín-Moreno, “In the diffraction shadow: Norton waves versus surface plasmon polaritons in the optical region,” *New J. Phys.*, vol. 11, p. 123020, 2009.

[520] V. E. Babicheva, S. Gamage, L. Zhen, S. B. Cronin, V. S. Yakovlev, and Y. Abate, “Near-field surface waves in few-layer MoS_2,” *ACS Photonics*, vol. 5, p. 2106, 2018.